UNIVERSITÀ DEGLI STUDI DELLA TUSCIA DI VITERBO

DIPARTIMENTO DI SCIENZE ECOLOGICHE E BIOLOGICHE

Corso di Dottorato di Ricerca in

Genetica e Biologia Cellulare - XXVII Ciclo

DOWN – REGULATION OF THE LAMIN A/C IN NEURONAL CELLS CORRELATES WITH IMMATURE PHENOTYPE

(BIO/11)

Tesi di dottorato di:

Dr. Marta Nardella

Coordinatore del corso

Prof. Giorgio Prantera

Tutore

Dr. Igea D'Agnano

8 maggio 2015

The best way to know God is to love many things

Vincent Van Gogh

To my parents,

my sisters

and my grandparents

To my husband

and

my son

INDEX

ABSTRACT

Le lamine nucleari sono proteine che appartengono alla classe dei filamenti intermedi di tipo V. Esse formano una struttura reticolare al di sotto della membrana nucleare interna e svolgono diverse funzioni, alcune delle quali non sono state ancora del tutto chiarite. Le lamine di tipo A sono espresse nei tessuti differenziati e sono coinvolte nei processi differenziativi che avvengono durante lo sviluppo embrionale. La loro espressione risulta ridotta o assente in molti tumori umani, tuttavia il loro ruolo nella tumorigenesi non è stato ancora caratterizzato. La perdita della Lamina A/C è di particolare interesse, poiché la progressione del tumore è spesso associata ad una regressione dello stato differenziativo delle cellule tumorali.

Nel nostro laboratorio è stato precedentemente dimostrato che la Lamina A/C è necessaria per il differenziamento delle cellule di neuroblastoma e che la sua perdita è associata ad un aumento dell'aggressività tumorale. Il neuroblastoma (NB) è un tumore altamente aggressivo del sistema nervoso autonomo ed è il più comune tumore solido extracranico in età pediatrica.

Nonostante l'identificazione di marker molecolari - come l'amplificazione del fattore di trascrizione MYCN - si sia rivelata molto utile dal punto di vista della stratificazione dei pazienti e della realizzazione di protocolli terapeutici, sono necessari nuovi target molecolari per rendere maggiormente chiara l'eterogeneità e la progressione del tumore.

Sulla base dei dati precedentemente ottenuti e considerando che la Lamina A/C si esprime esclusivamente nei tessuti differenziati, l'obiettivo del lavoro è consistito nell'individuare il ruolo della Lamina A/C nei processi di maturazione delle cellule di origine neuronale. In particolare, è stato osservato che l'assenza della Lamina A/C predispone le cellule a un fenotipo staminale, favorendo così lo sviluppo di cellule capaci di iniziare il tumore con le caratteristiche di auto-rinnovamento.

Inoltre, prendendo in considerazione il ben noto marcatore del NB, MYCN - normalmente amplificato nei tumori poco differenziati che mostrano caratteristiche immature - abbiamo esaminato la possibile esistenza di una relazione inversa tra LMNA e MYCN nel NB.

In questo studio abbiamo osservato una relazione inversa tra i livelli di espressione di LMNA e MYCN in 23 biopsie di NB. Utilizzando due modelli cellulari di NB che esprimono o LMNA o MYCN abbiamo dimostrato come questa correlazione inversa sia da attribuire ad un'alterazione del profilo di espressione di microRNAs che controllano la proliferazione e il differenziamento cellulare. Inoltre, abbiamo dimostrato che il silenziamento della Lamina A/C nelle cellule di NB SH-SY5Y comporta lo sviluppo di una popolazione di cellule inizianti il tumore (TIC), ovvero una

piccola popolazione di cellule responsabili della crescita del tumore, delle metastasi e delle recidive, nota come popolazione di cellule staminali tumorali. Tali cellule hanno molte caratteristiche specifiche delle cellule staminali - come la capacità di formare sfere e di espellere coloranti - ed esprimono marcatori di cellule staminali: POU5f, che codifica Oct4, Nanog, SOX2, nonché PROM-1, che codifica per CD133, e ABCG2. Inoltre, questa popolazione cellulare – diversamente da quella di origine – presenta un elevato potenziale tumorigenico in quanto le cellule sono in grado di generare un tumore quando inoculate in topi nudi. La caratterizzazione di NB TIC comporta un passo cruciale per il miglioramento delle terapie antitumorali.

Inoltre, come osservato nelle biopsie di NB, lo sviluppo di una popolazione di TIC in linee di NB correla all'incremento dei livelli di espressione del gene MYCN, come osservato in queste cellule. Infatti, sovraesprimendo MYCN, le cellule di controllo SH-SY5Y acquisiscono un fenotipo con caratteristiche staminali; al contrario, regolando negativamente i livelli di espressione di MYCN nelle cellule SH-SY5Y silenziate per Lamina siamo stati in grado di ripristinare il fenotipo più maturo.

Coerentemente con i nostri dati nei modelli di NB, il silenziamento della Lamina A/C nelle colture primarie di cervelletto di ratti neonati blocca la morte neuronale glutammato-mediata, che rappresenta un segnale della completa maturazione dei granuli cerebellari. Tale risultato rafforza l'ipotesi che l'espressione della Lamina A/C sia una caratteristica esclusiva delle cellule che iniziano il processo di maturazione e di quelle terminalmente differenziate.

Questo lavoro di tesi fornisce un modello di sviluppo di una popolazione di TIC nel neuroblastoma. Strategie mirate a colpire la popolazione di cellule staminali all'interno del tumore rappresentano una sfida per la riduzione della massa tumorale e/o dell'incidenza di recidive. Questi studi potrebbero consentire lo sviluppo di protocolli terapeutici personalizzati sulla base del profilo molecolare del singolo tumore.

Nuclear lamins are type V intermediate-filament proteins that form a meshwork-like scaffold underlying the inner nuclear membrane providing mechanical support to the nucleus. It is now clear that lamins exert many different functions within the cell, most of them still largely unknown. Among lamins, the A-type ones (Lamin A/C) are expressed in differentiated tissues and are involved in differentiation processes during the embryonal development. Their expression is reduced or absent in several human malignancies, even though their role in the tumorigenesis has not been characterized yet. It is widely accepted that tumor progression is often associated with regression from a more differentiated to a less differentiated state, therefore loss of Lamin A/C expression is of particular interest.

We previously demonstrated that Lamin A/C is necessary for the acquisition of a differentiated phenotype in neuroblastoma cells and its loss is associated to an increased cell aggressiveness.

Neuroblastoma (NB) is a highly aggressive embryonic tumor originating from the autonomic nervous system and represents the most common extracranial solid cancer in childhood. Despite the identification of molecular markers, such as MYCN amplification, turned out to be greatly useful in terms of patients' stratification and therapeutic protocols implementation, new molecular targets are required to clarify the heterogeneity and progression of this tumor.

Thus, based on our previous results and considering that Lamin A/C expression uniquely in differentiated tissues, we intended to examine a possible role of Lamin A/C in the maturation of cells of neuronal origin. In particular, we reasoned that NB differentiation impairment in the absence of Lamin A/C was mainly due to the acquisition of a stem-like phenotype and a concurrent development of tumor-initiating cells with self-renewal features. In addition, considering the well-known hallmark of NB MYCN, normally amplified in poorly differentiated tumors displaying immature characteristics, we intended to investigate whether an inverse relationship between LMNA and MYCN gene could exist in NB.

In this study, we observed an inverse relationship between LMNA and MYCN expression levels in 23 biopsies of NB. Using two NB cellular models, expressing LMNA or MYCN alternatively, we demonstrated that this inverse correlation is due to changes of members of miRNA signatures controlling cell proliferation and differentiation. Moreover, we provide evidence that the down regulation of Lamin A/C expression in the SH-SY5Y NB cells allows the development of a tumor-initiating cells (TIC) population, a rare tumorigenic cell population known to be responsible for sustaining tumor growth, metastases and relapse, and usually named cancer stem cell population. Stem cell characteristics, such as sphere-forming, dye exclusion ability and an increased expression of the stem cell regulatory network (POU5f, which encodes Oct4, NANOG and SOX2) as well as of PROM-1, encoding for CD133, and ABCG2 were detected in our TIC population.

Furthermore, TIC-derived tumors obtained after TIC cells implantation in nude mice showed a more malignant phenotype with respect to the parental cell line. The characterization of NB TICs may be a crucial step for the improvement of antitumoral therapies.

In agreement with the aforementioned NB biopsies, the development of a TIC population in NB correlates with the increased expression of MYCN gene observed in these cells. Indeed, by up-regulating MYCN, control cells acquired a stem-like phenotype; while down-regulating MYCN in the LMNA silenced cells, we were able to restore a more mature phenotype. Consistently with our data in the NB models, we also showed how Lamin A/C knock down in primary cells explanted from the cerebellum of neonatal rats prevents glutamate-mediated neuronal death which is a signal of the complete maturation of granule cells. This evidence strongly supports the idea that Lamin A/C expression is an exclusive characteristic of the cells that begin the maturation process and terminally differentiate.

This thesis work provides new mechanistic insight into the development of a stem-like NB TIC population. Targeting of the TICs in a tumor represents a challenge for the reduction of the tumor mass and/or the incidence of tumor recurrences. Therefore, our data may provide opportunities to develop new personalized therapeutic strategies based on the molecular profile of the tumor.

1 INTRODUCTION

1.1 ARCHITECTURE OF THE NUCLEUS AND IMPLICATIONS IN DISEASE

Nucleus and nuclear lamina

The nucleus is the defining feature of eukaryotic cells and is separated from the cytoplasm by the nuclear envelope (NE). The NE is composed of three distinct elements, i.e., the nuclear membrane, nuclear pore complexes, and the nuclear lamina. The nuclear membrane is a double-unit nuclear membrane, in which the outer nuclear membrane (ONM) is continuous with and shares biochemical and functional properties with the endoplasmic reticulum (ER). In contrast, the inner nuclear membrane (INM) is distinct from both the ONM and ER and is defined by a subset of integral membrane proteins, termed nuclear envelope transmembrane proteins (NETs) that are anchored to the INM during interphase. The ONM and INM are separated by a luminal space of 100 nm in width (perinuclear space). The nuclear membrane is punctuated by nuclear pore complexes (NPCs), which regulate the passage of macromolecules between the nucleus and the cytoplasm. At NPCs the ONM and INM converge at the so-called pore membrane, which again is defined by its own subset of integral membrane proteins. Underneath the INM is the nuclear lamina (NL). The NL is a polymeric protein meshwork of 10 nm filaments. It is a complex network of type V intermediate filaments (IF) proteins, the nuclear lamins, and inner nuclear membrane–associated proteins. The NL provides the mechanical and structural support for the nuclear membrane and anchoring sites for chromosomes and nuclear pore (Gerace and Burke, 1998).

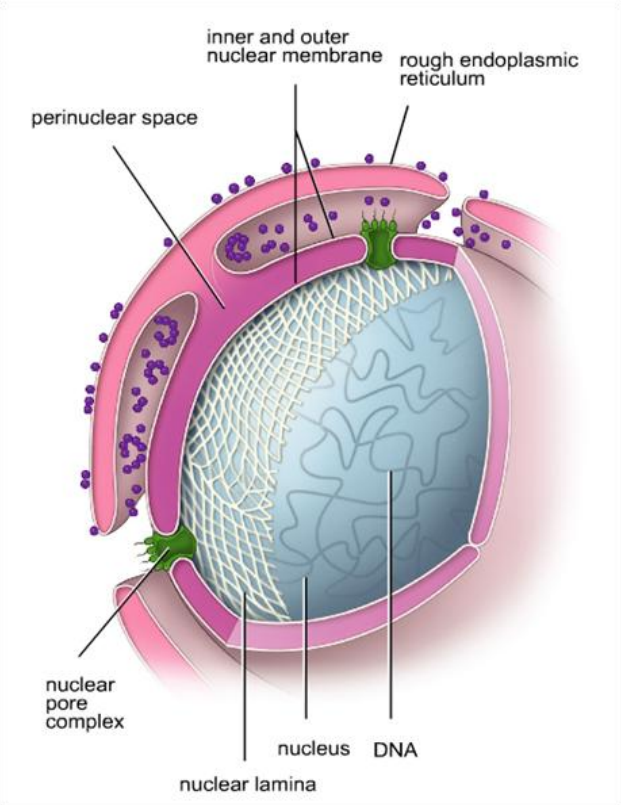

Schematic representation of nucleus structures.
http://www.slideworld.org/slideshow.aspx/Cytoskeleton-2865193

Nuclear lamins

The major components of the NL are type V intermediate filament (IF) proteins, the nuclear lamins. Like all proteins, they are synthesized in the cytoplasm and then transported into the nucleus, where they are assembled before being incorporated into the existing network of NL (Aebi et al., 1986).

Lamins are divided into A and B types based on sequence homologies. A-type lamins are 70 and 60 kilodaltons (Gerace and Blobel, 1980; Goldberg et al., 2008), are encoded by the LMNA gene located on chromosome 1q21.2-q21.3 (Wydner et al., 1996; Lin and Worman, 1997) and are generated by alternative splicing to produce different isoforms, lamins A, AΔ10, C and C2, which are all found in different cell types (Foster and Bridger, 2005; Martin et al., 2009). Lamin C2 is restricted only to spermatocytes during rat spermatogenesis whereas, AΔ10 is found only in a few carcinoma cell lines (Alsheimer and Benavente, 1996). AΔ10 results from the deletion of exon 10 (Hutchison, 2002) and is localised at the nuclear envelope (Broers et al., 1999).

The LMNA gene contains 12 exons. Exon 1 codes for the N-terminal head domain and the first part of the central rod domain of this gene. Exon 2-6 code for the central α-helical rod domain. Exons 7-9 code for the C-terminal tail domain for lamin A and lamin C. The nuclear localisation

signal (NLS) is contained in exon 7. Exon 10 contains a splicing site to generate lamin A and lamin C. Exon11 and 12 are specific for lamin A and coding for the CAAX box of pre-lamin A (Lin and Worman, 1993).

There are three types of B-type lamins (67 kilodaltons) in mammals: lamin B1, lamin B2 and lamin B3. Lamins B1 and lamins B2 are regulated and expressed in both embryonic and somatic cells during development whereas lamins B3 is regulated and expressed only in spermatocytes (Gerace and Blobel, 1980; Hutchison, 2002). Lamin B1 is encoded by LMNB1 and lamin B2 and lamin B3 are encoded by LMNB2 genes on chromosomes 5q23.2-q31.3 and 19p13.3, respectively (Lin and Worman, 1995; Dechat et al., 2008). LMNB1 gene contains 11 exons. Exon 1 codes for the N-terminal head domain and the first part of the central rod domain of this gene. Exon 2-6 code for the central α-helical rod domain. Exons 7-11 code for the C-terminal tail domain of lamin B. The nuclear localisation signal (NLS) is contained in exon 7. Exon11 contains a specific sequence for the CAAX box lamin B for post-translational farnesylation (Lin and Worman, 1993).

Little is known about the regulation of lamins gene expression. Some information are available on the regulation of LMNA gene expression. LMNA promoter presents different regulatory motifs among which a retinoic acid-responsive element (Okumura et al., 2000), binding sites for various transcription factors such as c-Jun, c-Fos and Sp1/3 (Okumura et al., 2004) or transcriptional coactivator such as CREB-binding protein (Janaki and Parnaik, 2006). Within the first intron of LMNA gene there are also binding sites for two transcription factors, the hepatocyte nuclear factor-3β and the retinoic X receptor β (Arora et al., 2004).

The nuclear lamins have a well-defined conserved domain structure consisting of an amino (N)-terminal globular domain, a central α-helical rod comprising four coiled-coil domains separated by linker regions L1, L12 and L2, and a globular carboxy (C)-terminal tail domain. Like the components of other intermediate filaments, the lamin alpha-helical domain is used by two monomers to coil around each other, indeed forming a dimer structure called “coiled coil”. Their assembly starts with the formation of coiled coil dimers which is associated with head to tail overlap. Two of these dimer structures then join side by side, in an antiparallel arrangement, to form a tetramer called “protofilament”. Eight of these protofilaments are laterally combined and twisted to form the characteristic 10 nm intermediate filament structure. These filaments can be assembled or disassembled in a dynamic manner. Although A- and B-type lamins interact each other *in vitro* (Sasse et al., 1998), little is known about their composition and structure in the cells within the lamina.

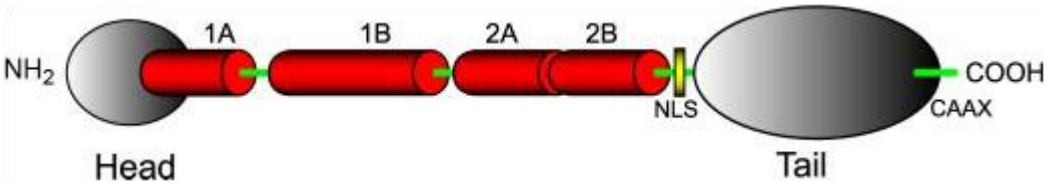

Schematic structure of lamin proteins.
Main characteristics are four central rod domains (1A, B, 2A, B), flanked by a globular head and a globular tail domain. In the globular tail domain, a nuclear localization signal (NLS) can be identified, as well as a CaaX motif, which is absent in lamin C but present in lamin A and in B-type lamins. Broers et al., Physiol Re, 2006.

The globular COOH-terminal domain of lamins shows an Ig-like structure. Between the COOH-terminal part of the rod domain and the Ig-like domain, lamins contain a nuclear localization signal sequence, not present in other IF proteins (Frangioni et al., 1993). Lamins, with the exceptions of lamins C and C2, are expressed as a pre-form and end in a C-terminal CAAX cassette which undergoes a highly structured sequence of posttranslational modifications before mature lamins are incorporated into the nuclear lamina. The CAAX cassette consists of a cysteine, two aliphatic amino acids and any COOH-terminal amino acid (Davies et al., 2009). The maturation process starts with farnesylation at the terminal cysteine site and is followed by cleavage of the last three amino acid residues of the CAAX motif and methylation of the carboxy-terminal cysteine. While the maturation of B-type lamins is terminated at this step, resulting in permanent farnesylation and carboxymethylation, an additional 15 amino acids are removed from the carboxyl terminus of farnesylated/carboxymethylated prelamin A. The last cleavage probably takes place during or after incorporation of this molecule into the nuclear lamina.

Besides farnesylation and carboxymethylation, during mitosis lamins are also posttranslationally modified by phosphorylation (Ottaviano and Gerace, 1985), sumoylation (Zhang and Sarge, 2008), ADP-ribosylation (Adolph et al., 1987), and possibly by glycosylation (Ferraro et al., 1989). In fact, during interphase the lamins are localised in the nuclear envelope resulting in a rim at the nuclear periphery and become dephosphorylated and polymerised at the nuclear periphery during telophase (Burke and Gerace, 1986; Foisner and Gerace, 1993).

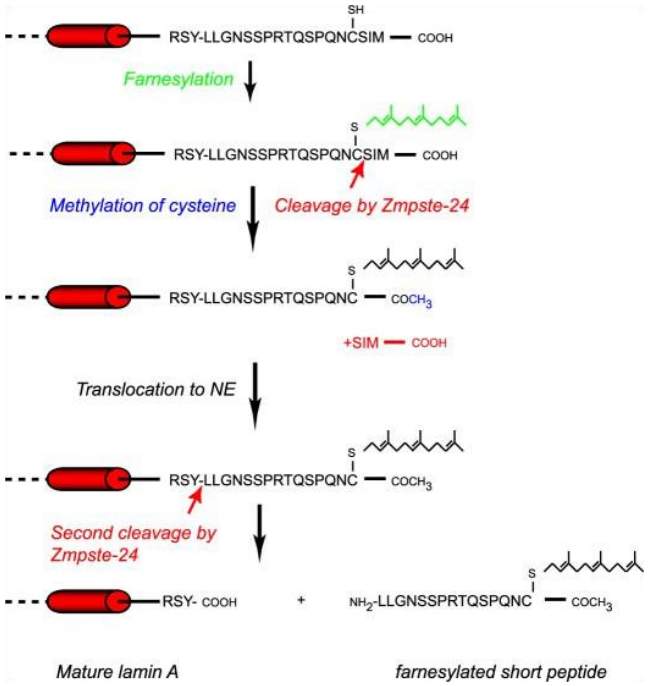

Post-translational processing of the carboxyl terminus of prelamin A.
Processing of prelamin A to mature lamin A involves several steps, including farnesylation at the terminal cysteine site, followed by cleavage of the last three COOH-terminal amino acid residues of the CAAX motif, in this case SIM, probably by Zmpste24; methylation of the cysteine that is COOH terminal after cleavage, followed by a second cleavage of the last 15 amino acids, including the newly added isoprene group. The last cleavage probably takes place during or after incorporation of this molecule into the nuclear lamina. Lamin C is not processed, whereas B-type lamins are farnesylated but not further processed. Broers et al., Physiol Re, 2006.

Functions of Lamins in Nuclear and cellular architecture

While the most obvious localization of lamins during interphase is at the nuclear periphery, a growing number of studies suggest that in interphase cells lamins can be found in nucleoplasmic areas as well. Three levels of lamin organization can be distinguished:

1) lamins associated with the nuclear membrane,

2) lamins organized into intranuclear tubules and aggregates,

3) lamins visible as dispersed (veil-like) structures in the nucleoplasm.

The roles of lamins are mediated by interactions with numerous lamin binding proteins both at the nuclear periphery and/or in the nucleoplasm. The lamins and associated NE proteins are scaffolds for proteins that regulate DNA synthesis, gene transcription, responses to DNA damage, cell cycle progression, cell differentiation, and cell migration (Broers et al., 2006; Verstraeten et al., 2007; Razafsky et al., 2014). There are many INM proteins binding to lamins either directly or indirectly. For example, INM proteins such as emerin, MAN1, LBR, LAP1, LAP2β, nesprin, otefin, and SUN1 have been demonstrated to bind lamins (Foisner, 2003). Lamins can also bind non

integral proteins including chromatin, histones (H2A/H2B; Höger et al., 1991), transcription factors such as E2F, RNA polymerase II transcription machinery (Mattout-Drubezki and Gruenbaum, 2003), pRb (Dorner et al., 2007), BAF (Barrier to Autointegration Factor; Furukawa, 1998), LAP2α, extracellular signal-regulated kinase (Erk), nuclear actin, and proteins of the nuclear pore complex such as nucleoporins (e.g. Nup153) (Vlcek et al., 2001; Mattout-Drubezki and Gruenbaum, 2003; Dechat et al., 2008; Olins et al., 2010). The actual *in vivo* interactions between lamins, DNA, chromatin and the INM remain unclear. However, interaction must be specific and reversible to allow nuclear growth and disassembly during mitosis. After mitosis and during interphase, the reorganization of nuclear lamina and its assembly at the nuclear periphery is elicited by the IMPs. Most of these proteins can bind directly to lamin A, lamin B or both (Wilson and Foisner, 2010).

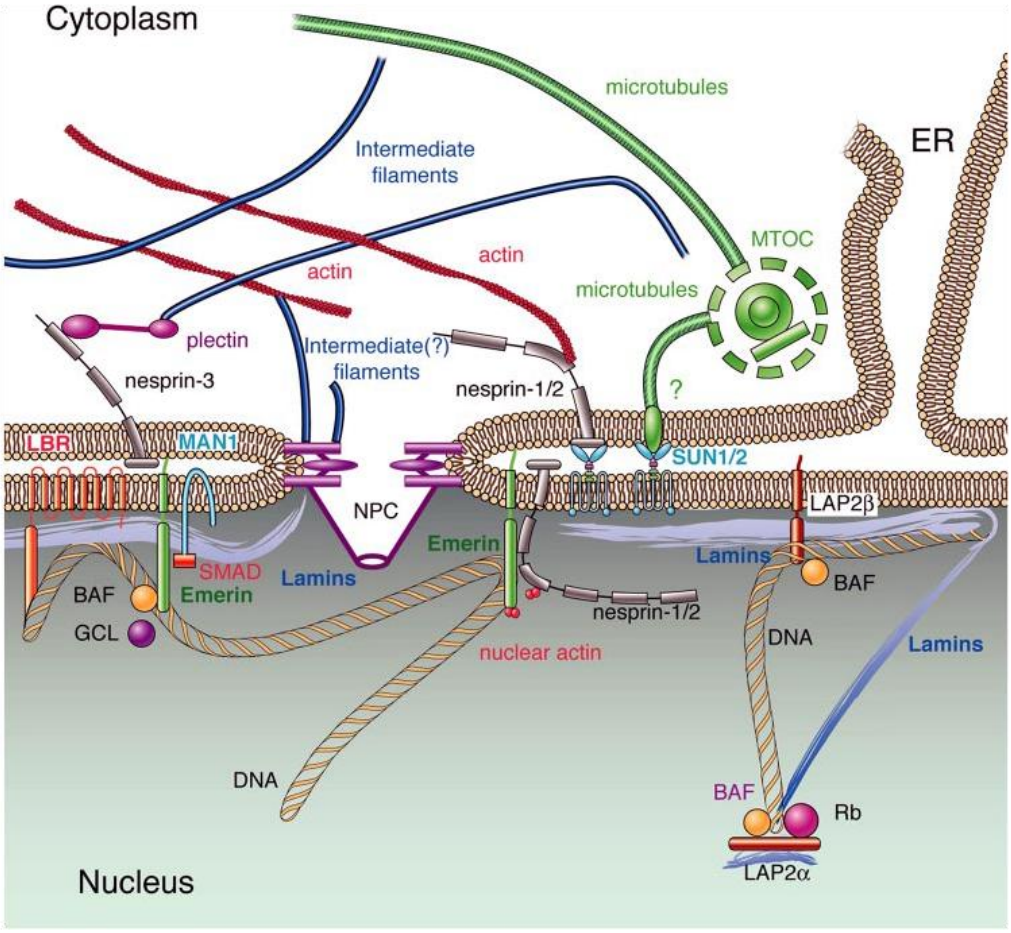

Model of the location of nuclear lamins and their interaction with nearby localized proteins.
Lamins bind directly to lamina-associated proteins (LBR, LAP2, emerin, MAN1, nesprins-1 and -2), but also to BAF, Rb, SREBP1, histone proteins, and DNA, and thereby mediate association with a scale of interacting structural proteins, including SUN1, actin, and possibly tubulin and intermediate filament proteins. Broers et al., Physiol Re, 2006.

Lamins/NET complexes have at least three clearly defined or emerging functions in maintaining cellular architecture. Lamin/NET complexes are important for organizing peripheral chromatin. The interaction between the lamins and chromatin involve their non-α-helical C-terminal tail domain and the N- and C-terminal tail domains of core histones (Mattout et al., 2007; Goldberg et al., 1999). Several proteins have been also described as lamin-binding proteins, which directly link both A- and B-types lamins to DNA (Schirmer and Foisner, 2007). Among these proteins are a Lamin B Receptor (LBR; Ye and Worman, 1994), the LAP2α protein, that binds specifically to Lamin A/C, the LAP2β protein, that interacts exclusively with B-type lamins (Dechat et al., 2000; Furukawa and Kondo, 1998), and BAF, which has been reported to bind to dsDNA and to histones (Margalit et al., 2007).

The lamins also have important functions in positioning NPCs within the NE, and have a crucial role in organizing the cytoskeleton. Specifically, the connection between the cytoplasm and nucleoplasm might be mediated by the interaction between SUN proteins (SUN1 and SUN2) and nesprins (nesprin-1, nesprin-2, and nesprin-3) in the luminal space (Padmakumar et al., 2005; Ketema et al., 2007). In the nucleoplasm Sun proteins interact with Lamin A (Haque et al., 2006), while in the cytoplasm, nesprins are thought to bind to actin (Warren et al., 2005) and possibly microtubules (Wiche, 1998). This assembly is referred to as the LINC complex (LInker of Nucleoskeleton and Cytoskeleton) and establishes a physical connection between the nucleoskeleton and the cytoskeleton (Crisp et al., 2006).

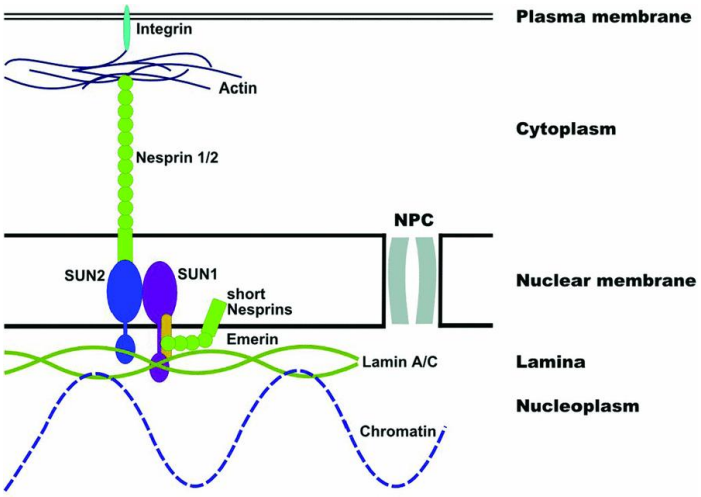

A model for the LInker of Nucleoskeleton and Cytoskeleton (LINC) complex.
Nuclear components, including lamins, bind to the inner nuclear membrane SUN domain proteins, which in turn bind to the KASH domain of the actin-associated giant nesprins on the outer nuclear membrane. The LINC complex establishes a physical connection between the nucleoskeleton and the cytoskeleton. Meinke et al., Biochem Soc Trans., 2011.

Lamins during development and differentiation processes

Different expression between nuclear Atype lamins and B-type lamins support the idea of their alternative functions during development and differentiation. The absence of lamin A/C in undifferentiated cells is responsible for the deformation of their nuclei. For example, lamin A is present in late embryos but not expressed in blastocysts whereas lamin A/C is expressed in oocytes (Prather et al., 1989; Bridger et al., 1993). Foster et al., in 2007, have shown that A-type lamins and B-type lamins are present at the nuclear envelope in early porcine embryos and that lamin A is also found in large intranuclear aggregates in two-cell to eight-cell embryos but is lacking in later embryonic stages (Foster et al., 2007). The regulated expression of A- and B-type lamins is also evident during differentiation of stem cells in culture. In fact, during the *in vitro* differentiation processes, human ES cells appear to express Lamin A/C before a complete down-regulation of the pluripotency marker Oct-4, suggesting that Lamin A/C expression is an early indicator of ES cell differentiation (Constantinescu et al., 2006). Differential expression of A- and B-type lamins has also been shown during neurogenesis in the adult rat brain (Takamori et al., 2007).

The developmental regulation of Lamin A/C expression has led various laboratories to hypothesize that these proteins play a role in differentiation. This has been recognized in muscle and adipocyte differentiation processes (Favreau et al., 2004, Frock et al., 2006, Lloyd et al., 2002; Hubner et al., 2006).

Lamins and diseases

Many aspects of nuclear as well as cytoplasmic activity are affected by modifications of the NE and the nuclear lamina. Processes as fundamental as DNA replication, transcription, and cell survival are altered in response to disruption of nuclear lamina, overexpression of mutant or truncated lamins, and loss-of-function mutations of the LMNA gene. Given the diversity of functions affected by these alterations, it is not surprising that complex patterns of tissue-specific pathologies are associated with lamin defects in humans. At present, no mutations in the Lamin B genes have been linked with human diseases, thus presuming that mutations in B-type lamins could be embryonic lethal. Conversely, A-type lamins have been in the limelight since the discovery that LMNA mutations or defective post-translational processing of pre–lamin A causes the majority of human diseases termed laminopathies, which include systemic disorders and tissue-restricted diseases (Capell and Collins, 2006; Verstraeten et al., 2007).

Classification and clinical phenotype of laminopathies

LAMINOPATHIES	CLINICAL MANIFESTATIONS
Systemic	
HGPS	Premature aging, hair loss, loss of subcutaneous fat, premature atherosclerosis, myocardial infarction, stroke
Atypical Werner's syndrome	Premature aging, cataracts, scleroderma-like skin changes, premature atherosclerosis, hair graying
Restrictive dermopathy	Intrauterine growth retardation, skin alterations, multiple joint contractures, skull defects
MAD	Skull/face abnormalities, clavicular hypoplasia, joint contractures/lipodystrophy, alopecia, insulin resistance
Tissue restricted	
EDMD	Early contractures of the neck/elbows/Achilles tendons, muscle contractures, wasting of skeletal muscle, cardiomyopathy with conduction disturbance
DCM	Ventricular dilatation, systolic dysfunction, arrhythmias, conduction defects
Limb-girdle muscular dystrophy 1B	Slowly progressive shoulder and pelvic muscle weakness/wasting,contractures, cardiac defects
Charcot-Marie-Tooth neuropathy type 2B1	Axonal degeneration, lower-limb motor deficits, walking difficulty, secondary foot deformities, reduced/absent tendon reflexes starting in the second decade of life
Dunningan-type FPLD	Dramatic absence of adipose tissue in the limbs/trunk and accumulation in the neck/face, hypertriglyceridemia, increased susceptibility to atherosclerosis/diabetes

To date, over 200 mutations from more than 1000 individuals have been identified in the LMNA gene, and a database on the nuclear envelopathies can be found at **http://www.umd.be**.

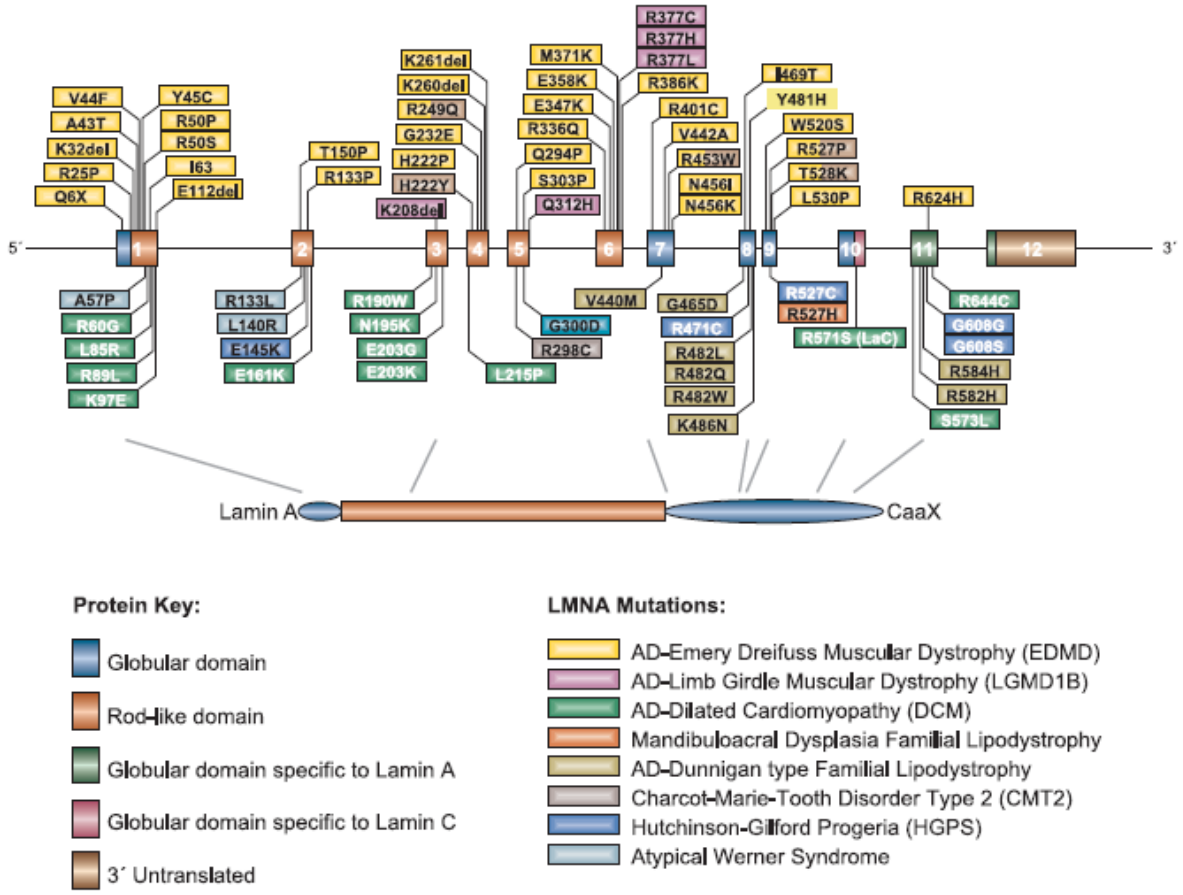

Different mutations in LMNA gene are associated with different diseases.
Most of the mutations resulting in the diseases affecting striated muscles are distributed throughout the gene. The majority of the mutations that result in Mandibuloacral disease, Dunnigan-type familial partial dystrophy, and Hutchinson Gilford Progeria syndrome cluster in the region of the LMNA gene encoding the C-terminal globular domain.

Lamins and cancer

Alterations in the nuclear lamina proteins are thought to be involved in malignant transformations and cancer processes because of their role as guardian of the genome, their role in regulating basic nuclear activities that are implicated in tumorigenesis, their interactions with cancer gene pathways and their role in chromosomal reorganization. Thus, lamin expression in cancer cells may serve as a biomarker for diagnosis, prognosis and tumor surveillance. The expression of the A-type lamins is often reduced or absent in various types of cancer and varies widely depending on the type of cancer, its aggressiveness, proliferative capacity and degree of differentiation. Changes in A-type lamins have been well documented in the current literature concerning various tumor types such as leukemia, lymphomas, some skin cancers, including basal cell and squamous cell carcinoma, adenocarcinoma of the stomach and colon, squamous and adenocarcinoma of the esophagus, small cell lung and prostate cancers, and testicular germ cell tumors (Stadelmann et al.,

1990; Broers et al., 1993; Moss et al., 1999; Venables et al., 2001; Oguchi et al., 2002; Coradeghini et al., 2006). In ovarian cancer cells, VEGF promotes the invasion, partially via the down-regulation of Ezrin and Lamin A/C caused by increased expression of miR-205 (Li et al., 2014). We have previously demonstrated that knockdown of Lamin A/C in human neuroblastoma cells inhibits retinoic acid-mediated differentiation and results in a more aggressive phenotype (Maresca et al., 2012).

In general, the expression of A-type lamins has been correlated with a non-proliferating, differentiated state of cells and tissues (Tilli et al. 2003). Given that tumor progression is often associated with regression from a more differentiated to a less differentiated state, loss of Lamins A/C expression may not be surprising. Even though the altered lamins expression are currently emerging as an additional event involved in malignant transformation and tumor progression, the role of A-type lamins in the tumorigenesis is not yet characterized and the molecular defects underlying the loss of A-type lamins in human cancer remain unknown.

Agrelo et al. (2005) has shown that CpG Island promoter hypermethylation of the LMNA gene is a significant predictor of poor outcome in some lymphomas (Agrelo et al., 2005). Cancer may also be considered an epigenetic disease and patterns of aberrant DNA methylation are now recognized to be a common hallmark of human tumors. Since A-type lamins present an important dual role as protector of chromatin from damage and as multifunctional regulators of gene transcription, the epigenetic silencing of LMNA gene in hematologic malignancies could aid understanding how lamin dysregulation could contribute to cellular transformation.

1.2 NEUROBLASTOMA

Neuroblastoma (NB) is an extra-cranial heterogeneous tumor of the sympathetic nervous system (Esiashvili et al., 2009). The first description of pediatric tumors under the term “neuroblastoma” was made by Dr. James Homer Wright of the Massachusetts General Hospital as early as 1910 (Modak et al., 2010). Today approximately 120 new cases are diagnosed in Italy each year, rendering this tumor the most common extra-cranial pediatric cancer. In 95% of cases, NB is diagnosed before the age of 5 years where it leads to 15% of all cancer-related fatalities in infancy and childhood (Mueller et al., 2009). Despite a century of extensive clinical and basic research efforts, the biology and clinical progression of the disease continues to present a multi-faceted clinical enigma in pediatric oncology. The most common site for primary NB tumors is the adrenal medulla; however, tumors can arise anywhere along the sympathetic branch of the autonomic

nervous system (Alam et al., 2009). At presentation, the disease can be limited to a single organ, locally or regionally invasive, or widely disseminated; more than 50% of cases are metastatic at presentation (Alam et al., 2009). The most common metastatic sites are lymph nodes, bone marrow, bone, and liver (Alam et al., 2009).

The clinical behavior of NB is highly variable, ranging from highly aggressive phenotypes to benign tumors with a high propensity for spontaneous regression (Brodeur, 2003). Intriguingly, NB is both disproportionally lethal despite very aggressive multimodal therapy and associated with a highest rate of spontaneous and complete regression in a subset of cases (Alam et al., 2009; Brodeur et al., 2003; Mueller et al., 2009).

Three broad risk categories (low, intermediate, and high risk) have been proposed on the basis of analysis of age at diagnosis, histology category, grade of tumor differentiation, DNA ploidy, and copy-number status at the MYCN oncogene locus at chromosome 11q. In particular the MYCN oncogene is target of high-level amplifications at chromosome band 2p24 observed in about 20% of NB and since such amplification has been found to profoundly affect the patients' clinical outcome, it is routinely used as prognostic biomarker and for treatment stratification (Seeger et al. 1111-16). MYCN belongs to a family of oncogenes called Myc oncogene-family members, whose most studied member is the MYC oncogene and include also MYCL oncogene. They are transcription factors, which activate, together with their dimerization partner Max, gene expression of a number of genes in an E-box dependent manner. MYCN and MYC probably have very similar molecular functions (Bonnet et al., 1997). The Myc oncogene-family members are involved in cell growth through protein synthesis, transcriptional regulation of ribosomal RNA processing, cell adhesion and tumor invasion.

Neuroblastoma as a sympathetic nervous system-derived tumor

The human nervous system consists of the Central Nervous System (CNS), comprising the brain and the spinal cord, and the Peripheral Nervous System (PNS), which links the CNS with the body's sense receptors, muscles, and glands. The PNS is divided in two components: the somatic or skeletal nervous system, which controls voluntary movement, and the autonomic nervous system, which regulates inner organ function via the sympathetic, parasympathetic or enteric ganglia.

The nervous system originates from the neural plate, an embryonic structure evolving from the ectodermal germ layer during the third week of gestation. During the process of neurulation, the neural plate invaginates ventrally and closes in order to form the neural tube, which will give rise to

the CNS. During this closure, neural crest cells originate at the interface between the closing neural tube and the dorsal ectoderm (LaBonne and Bronner-Fraser, 1999).

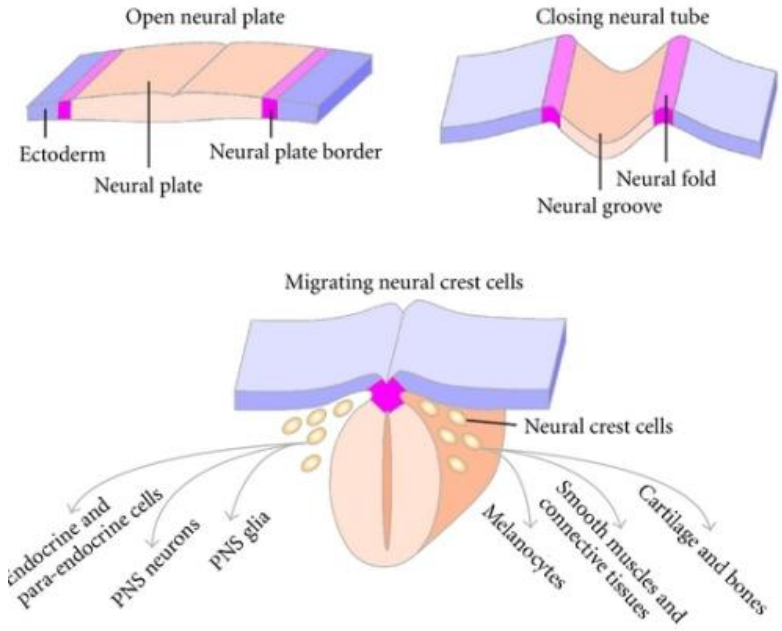

Nervous system development.
Invagination of the dorsal ectoderm, closure of the neural tube, neural crest formation at the interface of the closing neural folds and dorsal ectoderm, and migration of the pluripotent crest cells. Wislet-Gendebien et al., J Biomed Biotechnol., 2012.

The neural tube is initially composed of a single layer of cells. However, as development proceeds and extensive cell division occurs, the neural tube becomes multilayered, with precursor cells dividing in the medial portion of the neural tube adjacent to the central cavity, which will give rise to ventricles. The portion of the neural tube adjacent to the ventricles becomes the Ventricular Zone (VZ) and contains neural stem cells and dividing progenitors (Greene and Copp, 2009). These stem cell populations are capable of self-renewing through symmetric cell divisions or can differentiate through asymmetric cell divisions. The neural tube expands in the head of the embryo to form the brain and in the trunk to form the spinal cord. The early mammalian neural tube is a straight structure. However, even before the posterior portion of the tube has formed, the most anterior portion of the tube is undergoing drastic changes. In this region, the neural tube balloons into three primary vesicles: forebrain (prosencephalon), midbrain (mesencephalon), and hindbrain (rhombencephalon). By the time the posterior end of the neural tube closes, secondary bulges—the optic vesicles—have extended laterally from each side of the developing forebrain. The prosencephalon becomes subdivided into the anterior telencephalon and the more caudal diencephalon. The telencephalon will eventually form the cerebral hemispheres, and the

diencephalon will form the thalamic and hypothalamic brain regions that receive neural input from the retina. Indeed, the retina itself is a derivative of the diencephalon. The mesencephalon does not become subdivided, and its lumen eventually becomes the cerebral aqueduct. The rhombencephalon becomes subdivided into a posterior myelencephalon and a more anterior metencephalon. The myelencephalon eventually becomes the medulla oblongata, whose neurons generate the nerves that regulate respiratory, gastrointestinal, and cardiovascular movements. The metencephalon gives rise to the cerebellum, the part of the brain responsible for coordinating movements, posture, and balance (Gilbert, 2000).

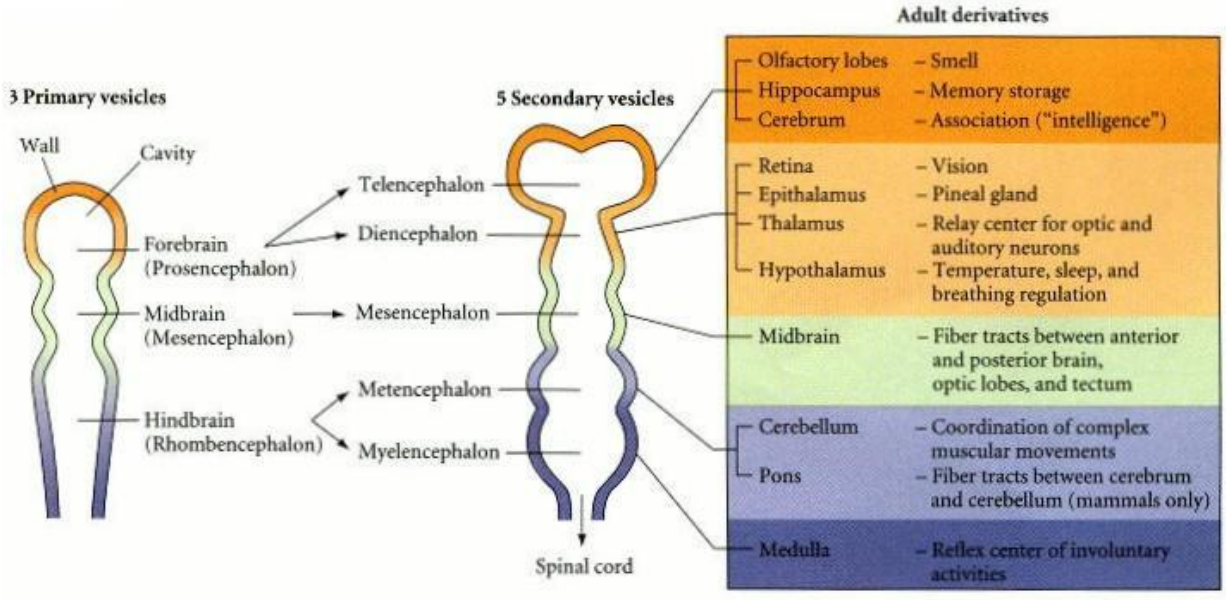

Early human brain development.
The three primary brain vesicles are subdivided as development continues. On the right is a list of the adult derivatives formed by the walls and cavities of the brain. Gilbert, 2000.

The cerebellum is one of the best studied parts of the brain. The cerebellar cortex is composed of four main types of neurons: granule cells (GCs, the most numerous neurons of the entire central nervous system), Purkinje cells (PCs) and two types of inhibitory interneurons, the Golgi cells and the stellate/basket cells. The cerebellum develops over a long period, extending from the early embryonic period until the first postnatal years. The main cell types of the cerebellum arise at different times of development and at different locations. The PCs and the deep cerebellar nuclei arise from the ventricular zone of the metencephalic alar plate, whereas the GCs are added from the rostral part of the rhombic lip, known as the upper rhombic lip. The rhombic lip, is the dorsolateral part of the alar plate, and it forms a proliferative zone along the length of the hindbrain. Cells from its rostral part reach the superficial part of the cerebellum, and form the external germinal or granular layer (EGL) at the end of the embryonic period. Granule cells are formed in the EGL. The

granule cells form axons, the parallel fibres, and migrate along the processes of Bergmann glia cells (BGCs) to their deeper, definitive site, the internal granular layer (IGL). In the fetal period, the IGL is formed by further proliferation and migration of the external germinal cells. This layer, situated below the layer of Purkinje cells, is the definitive granular layer of the cerebellar cortex. A transient layer, the lamina dissecans, separates the IGL from the Purkinje cells. Ultimately, it is filled by migrating granule cells and disappears (Rakic and Sidman, 1970). During the inward migration of the postmitotic granule cells (16–25 weeks), the Purkinje cells enlarge and develop dendritic trees (Milosevic and Zecevic, 1998; Miyata et al., 1999). The EGL appears at the end of the embryonic period and persists for several months to 1–2 years after birth (Lemire et al., 1975).

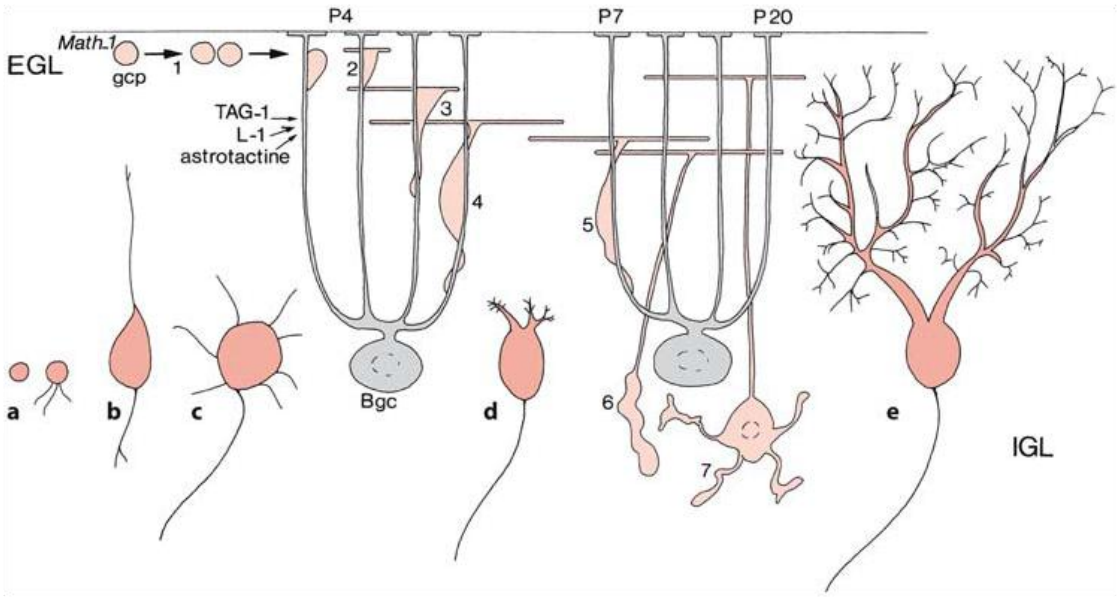

Differentiation of cerebellar cortical neurons.
GCs (light red) arise (1) from granule cell precursor cells (GCPs) in the external granular layer (EGL), migrate in several steps (2 – 7) along the dendrites of Bergmann glia cells (BGCs) to the internal granular layer (IGL).The development of PCs (red) also involves several steps (**a** – **e**). Hatten et al., Curr Opin Neurobiol., 1997.

Neural crest cells delaminate from the neural tube and migrate extensively throughout the embryo to generate, differentiate, and populate numerous organs. During this migration, neural crest cells undergo differentiation and form Schwann or glial cells, melanocytes, and sympathoadrenal progenitor cells. From these sympathoadrenal progenitor cells is derived the sympathetic nervous system (SNS). SNS's special feature relates to the organism's "fight or flight" response. There are three types of cells present in the SNS: chromaffin cells (adrenal medullary cells), small intensely fluorescent cells, and sympathetic neurons (known as neuroblasts during embryogenesis). The migrating neural crest cells are influenced by the molecular guidance given by various external factors and ligands acting on the receptors present on the surface of the neural crest cells. The morphology, differentiation, and derivatives of the neural crest cells are also mediated by

local tissue interactions. Genetically regulated cell-autonomous factors or exposure to environmental factors result in disturbances of differentiation, which then give rise to uncontrolled cell cycle or ectopic tissue formation. Disturbances in neural crest cell regulation are involved in different serious diseases such as neuroblastoma (Takahashi et al., 2013; Etchevers et al., 2006).

1.3 CANCER STEM CELLS AND NB-TUMOR INITIATING CELLS

The cancer stem cell theory

To explain the initiation and development of tumors two alternative models have been proposed: the stochastic model and the hierarchical model. The stochastic model posits that the tumors are composed of heterogeneous cells and all the cells have the potential to be a tumor-founding cell. In contrast, the hierarchical model proposes that malignancies are formed of a hierarchy of cells and are driven by rare subpopulation of cells referred to as cancer stem cells (CSC) or tumor initiating cells (TIC). Only this subset of cells in the tumor has the potential to form tumors (Vescovi et al., 2006).

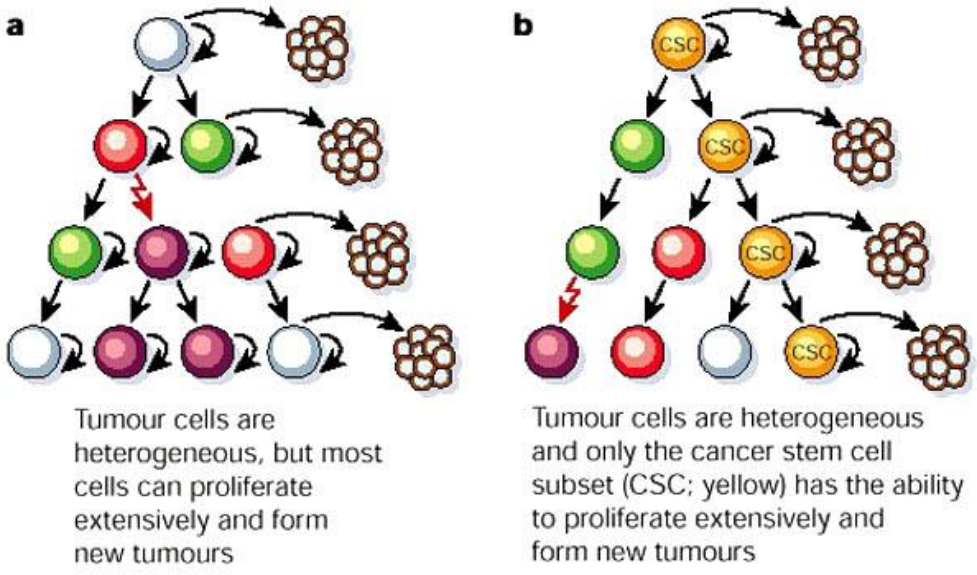

Comparison between the stochastic model and the CSC model for tumor growth.
a) In the stochastic model, oncogenic events (represented by lightning bolts) in one or multiple clones give these cells a growth advantage. **b**) In the CSC model only a distinct subset of cells have the potential to proliferate extensively and form new tumors. Most of the cells lack this ability. Reya et al., Nature; 2001.

CSCs are defined as a subset of tumorigenic cells that are endowed with enormous proliferative, clonogenic, self-renewal, and multi-lineage differentiation potentials *in vitro* and tumor-initiating ability in immune-deficient animals such as NOD/SCID mice (Clarke et al., 2006; Tang et al., 2007; Visvader et al., 2008; Rosen et al., 2009).

CSCs, like their normal counterparts, possess two important and fundamental properties, which are self-renewal and differentiation. Self-renewal is the ability for CSCs to undergo symmetric division and replenish the cancer stem cell pool. During differentiation, CSCs may undergo asymmetric or symmetric division, therefore giving rise to the multi-lineage of differentiated cells that comprise the heterogeneous populations of cancer cells.

The experimental premise of the cancer stem cell theory is based on the ability to purify CSCs on their physical and/or functional characteristics, such as cell surface marker expression (CD133, CD34) or dye exclusion ability (Fábián et al., 2009; Patrawala et al., 2005). A second imperative requirement to study CSC biology is the development of a reliable assay to quantify CSC tumorgenicity and proliferation. Current standard *in vivo* assays employ immunocompromised rodents such as non-obese diabetic/severe combined immunodeficiency (NOD/SCID) or NOD/SCID interleukin-2 receptor gamma chain null (Il2rg-/-) mice for xenografts of human cancer cells (Quintana et al., 2008; Dick et al., 1991).

Using the aforementioned techniques, the first cancer type upon which the CSC theory has been established is acute myeloid leukemia (AML) (Bonnet et al., 1997). Since 2003, putative CSCs have been reported for many human solid tumors including brain tumor, breast, colon, pancreatic and prostate cancers (Singh et al., 2004; Schatton et al., 2008; Al-Hajj et al., 2003; O'Brien et al., 2007; Dalerba et al., 2007; Li et al., 2007; Hermann et al., 2007).

The cancer stem cell theory predicts that unless the cancer stem cell pool is eradicated by a given set of therapeutic approaches, the cancer will recur. It is believed that CSCs are inherently more resistant to standard therapies. This feature can in part be attributed to their functional similarities with normal stem cells (Pallini et al., 2008). Conversely, therapeutic targeting of these CSCs will give promising results with reduction in tumor mass and/or incidence of tumor recurrence (Piccirillo et al., 2006).

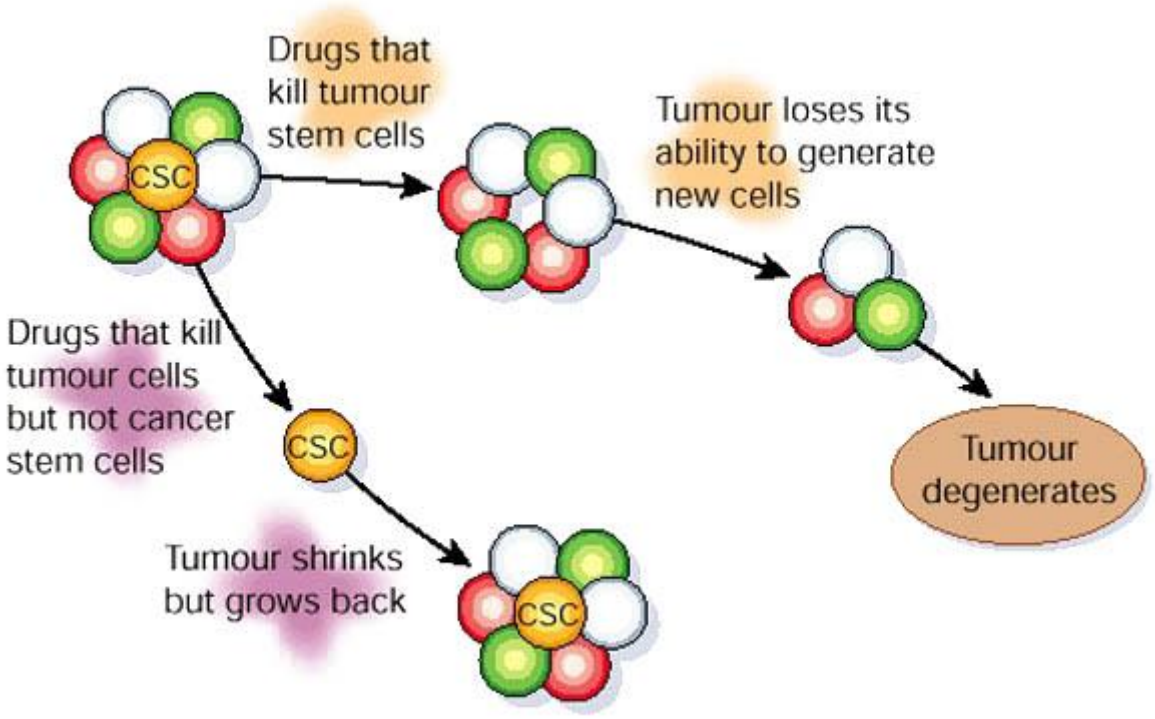

Cancer stem cell theory.
Conventional therapies usually target cells with limited proliferative potential which results in shrinkage of tumor. As the putative cancer stem cells escape these therapies, ultimately the tumor is re-established. In contrast, therapies targeting the CSCs result in loss of tumors ability to regenerate and grow. Reya et al., Nature; 2001.

Isolation and characterization of neuroblastoma tumor initiating cells

Extensive metastases and frequent relapse in NB patients following aggressive treatments gave rise to early hypotheses that NB contains a set of cells that were inherently more resistant to therapeutic regiments and had the self-renewal, proliferation and differentiation properties of cancer stem cells. In 2007, Hansford et al isolated a highly tumorigenic population of sphere-forming cells from bone marrow aspirates of low and high-risk NB patients with metastatic disease (Hansford et al., 2007). This population, termed NB tumor-initiating cells (NB-TICs), were expanded under serum-free neurosphere growth conditions containing basic fibroblast growth factor, epidermal growth factor and B27, a multi-factor neuronal growth supplement. Similar to brain, breast and colon CSCs, NB-TICs proliferate as suspension spheres *in vitro*. Furthermore, NB-TICs express neuroblastoma markers NB84 and tyrosine hydroxylase as well as the neural crest marker nestin and have genetic alterations commonly seen in neuroblastoma, further establishing this population as neuroblastoma-lineage cells (Hansford et al., 2007). Introducing genetically engineered oncolytic virus is the next generation anticancer therapy. Mahller et al (2009) used nestin-targeted oncolytic

herpes simplex virus (HSV), which killed TICs in neuroblastoma and also prevented the formation of the tumors in athymic nude mice (Mahller et al., 2009).

The identity of TICs in NB *in vivo* is not yet fully recognized because of their cellular heterogeneity, which is a significant feature of neuroblastoma. Seventeen cell lines have been studied and among them the existence of three different cell types was observed, which has been named N-type (neuroblastic), I-type (intermediate type), and S-type (substrate-adherent) cells (Rettig et al., 1987). N-type cells have neuritic processes, scant cytoplasm, neurofilaments, granin, pseudoganglia, and expression of neurotransmitter enzymes. S-type cells have extensive cytoplasm, vimentin, and CD44 expression. I-type cells express features of both N-type cells and S-type cells. I-type cells are significantly more malignant than N- or S-type cells, with four- to five-fold greater plating efficiencies in soft agar and six-fold higher tumorigenicity in athymic mice (Walton et al., 2004).

These striking characteristics have led to the suggestion that I-type cells represent neural crest cancer stem cells and, therefore, embody the truly tumourigenic component of neuroblastoma (Ross et al., 1995).

The presence of highly malignant CSCs could significantly diminish patient prognosis and long term survival. Indeed, it has been demonstrated that tumours identified as high–risk or exhibiting progressive disease contain a higher fraction of I-type cells than low-risk tumors . Cell-cell interaction between the different phenotypic cell variants can influence tumor viability, tumourigenicity and even response to therapy (Ross et al., 2003).

1.4 microRNAs

MicroRNAs (miRNAs) are evolutionally conserved, small non-coding RNAs that are about 19-22 nucleotides (nt) long. miRNAs modulate gene expression by repressing their targets' translation or inducing mRNA degradation through binding to the complementary sequence in target messenger RNA. miRNAs are annotated and catalogued in the public-accessible web-based database miRBase (www.mirbase.org), which was founded at the Sanger Institute in England and is now managed by the University of Manchester. So far, 1881 mature miRNAs have been reported in humans (miRbase, Kozomara and Griffiths-Jones, 2014). The miRNA nomenclature is managed by miRBase and has been slightly changed with upcoming releases of the database. In general, miRNA names start with a 3-4-letter prefix to designate the species (e.g. hsa- for homo sapiens miRNAs). They are further assigned by a three-letter prefix, such as miR- or let-, followed by a sequential number (e.g., miR-1). By definition, the mature miRNA is labeled "miR" (Griffiths-Jones et al.,

2006) while the precursor is labeled “mir”; however, this discrimination is not stringently used in the literature, and it has been recommended to use “mature” or “precursor” when a clear distinction is necessary. Identical miRNAs transcribed from different genes are given a numeric suffix, e.g. miR-1–1 and miR-1–2. Very similar miRNAs (paralogous miRNAs), often sharing the same seed sequence, are designated as a “miRNA family” (e.g. mir-29 family) and discriminated by numeric and letter suffixes (e.g. mir-29a, mir-29b, mir-29c; Ambros et al., 2003). In some cases, two mature miRNAs are processed from the same stem-loop precursor, one from each arm, and are accordingly designated by an additional suffix “-5p” (for that released from the 5’-arm) and “-3p” (for that released from the 3’-arm); e.g., miR-199a-5p and miR-199a-3p. The star-forms (miR*), previously used for minor forms, have been “retired” according to the latest nomenclature convention (Kozomara et al., 2011).

miRNA biogenesis

The biogenesis of miRNAs is a complex multi-step process that starts in the nucleus and ends in the cytoplasm of cells. Most miRNAs are transcribed as long monocistronic or polycistronic primary transcription units (primary miRNA or pri-miRNA) by RNA polymerase II. Typically, a pri-miRNA is characterized by a hairpin structure, containing a double-stranded (ds) RNA stem of ~33 base pairs (bp), a terminal loop, and single-stranded (ss) RNA flanking regions. The stem-loop structure contains the miRNA in the 5’ or 3’ half of the stem. The pri-miRNA is cleaved in the nucleus by a protein complex (the “microprocessor complex”) consisting of several proteins including the RNase III enzyme, Drosha and its co-factor DGCR8. DGCR8 functions as a molecular anchor and defines the binding site for the microprocessor, while Drosha cleaves the RNA approximately 11 bp from the ss-dsRNA junction, producing the shorter, ~ 65-70-nucleotide long hairpin pre-miRNA.

Following completion of this nuclear processing step, the pre-miRNA is exported from the nucleus to the cytoplasm by the Exportin-5. Here, the pre-miRNA is cleaved by another RNAse III enzyme called Dicer. Dicer cleaves ~22 nt from the pre-existing end of the pre-miRNA, producing ~22 nt double-stranded RNA molecules. One of the two strands (the guide strand or mature miRNA) is, selected upon thermodynamic properties, loaded on an Argonaute (Ago) protein, the main constituent of the RNA-Induced Silencing Complex (RISC). The other strand (passenger strand) is degraded. The mature miRNA sequence guides the RISC complex to recognize and target partial complementary mRNA sequences, primarily within the 3’-untranslated region (3’UTR) (Kim et al., 2009; Siomi et al., 2009; Guarnieri et al., 2008).

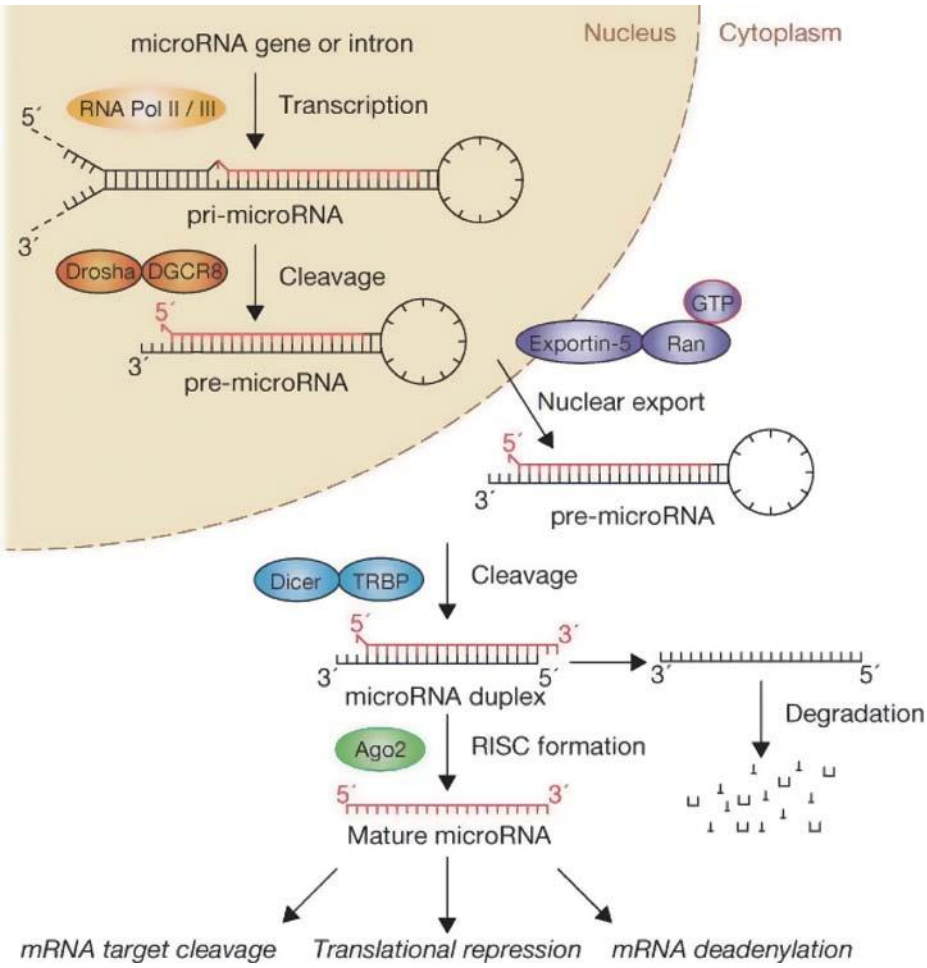

miRNA biogenesis pathways and function in gene regulation.
Winter et al., Nature Cell Biology; 2009.

The mechanisms of miRNA-mediated post-transcriptional regulation on target mRNAs include blocking the translation and/or inducing the degradation of mRNAs by deadenylation and decapping processes ("mRNA-destabilization scenario"). No matter which mechanism predominates, the overall output is the reduction of amount of protein encoded by the target messenger (Bartel, 2009).

As miRNAs tend to target many different mRNAs, and each mRNA may contain several to hundreds of different miRNA binding sites, it is obvious that the miRNA-mRNA regulatory network is extremely complex. It has been estimated that 30-60 % of all human genes are regulated by miRNAs (Lewis et al., 2005; Friedman et al., 2009). miRNA regulation is involved in almost all physiological processes, including stem cell self-renewal, differentiation, proliferation, metabolism, survival and death pathways (Guarnieri et al., 2008; Huang et al., 2011). As a consequence of this broad function, miRNA biogenesis has to be tightly controlled. Good functionality of the nuclear membrane and in particular nuclear lamins could play a crucial role in biological functions such as

miRNA processing. Deregulated miRNA expression has been associated with a variety of diseases, including cancer. Changes in the composition of the nuclear membrane occur during the progression of several types of cancers that could be associated to miRNA deregulation (Park et al., 2009; Weber et al., 2010). Furthermore, miRNA transcription is regulated by several transcription factors, including oncogenes like MYCN.

miRNAs may function as oncogenes or tumor suppressor genes in NB

Chen and Stallings demonstrated that miRNAs play a role in NB pathobiology (Chen et Stallings, 2007). The aberrant expression of miRNAs in NB suggests that these miRNAs may function as either oncogenes or tumor suppressor genes. For example, Fontana et al demonstrated that the five miRNAs mapping within the miR-17--92 polycistronic cluster (miR-17-5p, -18a, -19a, -20a and -92) were expressed at high levels in NB cell lines (Fontana et al., 2008). High expression of miR-17-92 cluster promotes several aspects of oncogenic transformation, including inhibition of apoptosis and oncogene-induced senescence (Hong et al., 2010), by targeting p21 WAF1, pRB and E2F1 (Cloonan et al., 2008; Hong et al., 2010). Moreover, recently it was shown that miR-20a, miR-9 and miR-92a, which are critical for cell differentiation and are modulated by MYCN oncogene, are able to modulate the apoptotic program at the early stage of NB differentiation by regulating the expression of various apoptosis-related genes (Guglielmi et al., 2014).

On the other hand, many miRNAs that are under-expressed in NB might exert tumor suppressor functions. For example, miR-34a functions as a potential tumor suppressor by inducing apoptosis in NB cells. miR-34a directly targets the mRNA encoding E2F3 and significantly reduces the levels of E2F3 protein, a potent transcriptional inducer of cell-cycle progression (Christoffersen et al., 2010). Other important tumor suppressive miRNAs include mR-101, which targets the proto-oncogene MYCN and inhibits cell proliferation in MYCN-amplified NB (Buechner et al., 2011).

miRNA regulation of CSC

Increasing evidences have suggested that miRNAs might be involved in regulating CSC properties, including self-renewal and differentiation, tumorigenesis, metastatic potential and chemoresistance. First, miRNA signature specific for CSC populations has been reported in several cancers. In breast cancer, Yu et al. reported that let-7 as well as a number of other miRNAs including miR-16, miR-107, miR-128 and miR-20b were significantly reduced in breast CSCs (BCSC) enriched by consecutively passaging breast cancer cell line SKBR3 in mice treated with

chemotherapy (Yu et al., 2007). Clarke's group used the cell surface CD44 and CD24 marker expression to enrich BCSC, and identified a set of 37 miRNAs to be differentially expressed in $CD44^{+}/CD24^{-/lo}$ BCSC population, in which three clusters, miR-200c-141, miR-200b-200a-429, and miR-183-96-182 were significantly downregulated (Shimono et a., 2009). miRNA deregulation has also been reported in glioblastoma and other brain CSCs (Gal et al., 2008, Godlewski et al., 2009; Garzia et al., 2009). For example, by comparing miRNA expression in $CD133^{+}$ glioblastoma stem cells with the $CD133^{-}$ population, Gal et al. showed that miR-451 as well as miR-486, miR-425, miR-16, miR-107 and miR-185 level were increased in the $CD133^{-}$ population (Gal et al., 2008). In hepatic CSCs identified by $EpCAM^{+}AFP^{+}$ profile, researchers also discovered a unique miRNA signature in which miR-181 family and several miR-17-92 cluster members were up-regulated in the CSC population (Ji et al., 2009).

Several studies have reported that miR-155 is involved in one most critical step in the metastatic cascade, epithelial-mesenchymal transition (EMT). EMT is a remarkable example of cellular plasticity that involves the dissolution of epithelial tight junctions, the intonation of adherens junctions, the remodeling of the cytoskeleton, and the loss of apical-basal polarity. In cells undergoing EMT, the loss of epithelial cell adhesion and cytoskeletal components is coordinated with a gain of mesenchymal components and the initiation of a migratory phenotype (Wang et al., 2003; Zavadil et al., 2007). Kong et al. reported that miR-155 plays an important role in TGF-beta-induced EMT, cell migration and invasion by targeting RhoA, disrupting tight junction formation (Kong et al., 2010).

2 AIM

Based on our previous data showing that Lamin A/C is necessary for the differentiation of neuroblastoma cells and its loss is associated to increased cell aggressiveness, and considering that Lamin A/C is expressed uniquely in differentiated tissues, I intended to identify a role of Lamin A/C in the maturation of cells of neuronal origin.

I hypothesize that the lack of Lamin A/C could predispose cells toward a stem-like phenotype, thus influencing the development of tumor-initiating cells (TICs) with self-renewal features in neuroblastoma. In a tumor-mass, TICs constitute a rare tumorigenic cell population responsible for sustaining tumor growth, metastases and relapse. Moreover, the amplification of the MYCN gene, encoding for a known transcription factor, is one of the most important molecular features in neuroblastoma, correlating with rapid disease progression and poor prognosis. Hence, considering a possible opposite role of the LMNA and the MYCN genes I intended to investigate whether an inverse relationship between LMNA and MYCN gene expression could exist in neuroblastoma. In particular, I hypothesized a possible reciprocal regulation between the two genes mediated by microRNAs.

To address this hypothesis I used as experimental model the SH-SY5Y and LAN-5 human neuroblastoma cell lines expressing LMNA or MYCN alternatively. We also employed the SH-SY5Y model in which we have previously silenced LMNA gene.

3 MATERIALS AND METHODS

Human NB biopsy RNA extraction and real-time RT-PCR

Total RNA was extracted from twenty-three frozen biopsies of human newly diagnosed NBs obtained from Department of Pediatrics and Infantile Neuropsychiatry of Sapienza University, Rome using TRIzol reagent (Life Technologies) according to the manufacturer's instructions. RNA was reverse-transcribed, and real-time PCR performed as described above. Institutional written informed consent was obtained from the patient's parents or legal guardians according to the local institutional guidelines.

Cell line maintenance and sphere formation

The SH-SY5Y NB cell line was purchased from ATCC. In this study, we also used two SH-SY5Y-derived clones, LMNA-KD and control (CTR) cells that were grown as previously described (Maresca et al., 2012). The LAN-5 NB cell line (a gift from Dr. Doriana Fruci) was grown in RPMI-1640 medium (Gibco) supplemented with 10% FBS (Hyclone), 2 mML-glutamine and 1% penicillin/streptomycin in a fully humidified incubator containing 5% CO_2 at 37°C. To obtain spheres, cells were plated in a serum-free media in 60-mm, low-attachment culture dishes at a density of $9.5x10^5$ cells/cm^2 and cultured in Neurobasal Medium (Gibco) supplemented with 20 ng/ml Epidermal Growth Factor (EGF, Sigma), 40 ng/ml basic Fibroblast Growth Factor (bFGF, Sigma), 1% neuronal supplement N2 (Gibco) and B27 (Gibco), and 2 µg/ml heparin. Three days after seeding, the cells formed floating neurosphere-like structures that grew rapidly until day 7. Before these structures became necrotic, we harvested and suspended them in Accutase enzymatic solution (Gibco) for 5 min at 37°C and then mechanically dissociated into a single-cell suspension. The cells were re-seeded in the same conditions as above, and the secondary spheres were allowed to form. As positive and negative controls, we used NB LAN-5 and SH-SY5Y cell lines, respectively. TICs were derived by harvesting the secondary spheres, treating them with Accutase enzymatic solution (Gibco) for 5 min at 37°C and then mechanically dissociating them into a single-cell suspension. These cells were seeded in adherent conditions in the presence of 1:1 mixture of Eagle's Minimum Essential Medium and F12 medium (Gibco) supplemented with 10% FBS (Hyclone), 2 mM L-glutamine, 0.5% non-essential amino acids, 0.5% sodium pyruvate and 1% penicillin and streptomycin.

Primary cell coltures of Granule Cells

Cultures enriched in granule neurons were obtained from dissociated cerebella of 8-day-old Wistar rats (CGC; Charles River, Calco, Italy) according to the procedure described by Levi et al. (1984). Cells were seeded (3 x 10^6 cells/dish) on poly-L-lysine-coated 35-mm plastic dishes (NUNC, VWR International PBI s.r.l., Milano, Italy) in basal medium Eagle (BME; Life Technologies, Gaithersburg, MD, USA) supplemented with 10% heat-inactivated fetal calf serum, 2 mM glutamine and 25 mM KCl and 100 µg/ml gentamycin (Life Technologies, Gaithersburg, MD, USA). Ara-C (10 mM) was added to the culture medium 24 h after plating to prevent proliferation of nonneuronal cells.

Generation of Lentiviral Infection of Granule Cells

The cells were seeded into 35-mm plastic dishes previously coated with poly-L-lysine at a concentration 3,5 x 10^5 cells/dish. After four hours, the cells were infected for 18 hours with the virus-containing supernatant from pLenti6/V5-GW/EmGFP-miR-LMNA or pLenti6/V5-GW/EmGFP-miRNeg (Maresca et al. 2012), and then fresh medium was added. The miRNA expression was monitored by checking the simultaneous coexpression of the EmGFP reporter gene by fluorescence microscopy.

Glutamate toxicity and neuronal survival

After 2, 5 and 8 days in culture, cells were washed once in Locke solution (in mM: 154 NaCI, 5.6 KCI, 3.6 NaHC03, 2.3 CaC12, 1.0 MgC12, 5.6 glucose, 10 HEPES, pH 7.4) and exposed at room temperature to a 100 µM glutamate pulse in Mg^{2+}-free Locke solution for 30 min. Cells were subsequently washed in Mg^{2+}-free Locke solution, replenished with their original medium and returned to the incubator. After 18 h, viable cells were assessed by counting the numbers of intact nuclei as described by Soto and Sonnenchein (1985), modified for counting cerebellar granule cells by the procedure of Volontè et al. (1994). This method has been shown to be reproducible and accurate and to correlate well with other methods of assessing cell survival-death (Stefanis et al. 1997; Stefanis et al. 1999). Cell counts were performed in triplicate and are reported as means ± SEM. The data are expressed as the percentage of intact nuclei in the control cultures at each time point.

Colony-forming assay

The LMNA-KD and sphere-derived adherent cell line were seeded at decreasing clonal densities (range: 15–1,000 cells/dish) in 60-mm Petri dishes. Fifteen days after seeding, the cells were fixed for 10 min in ice-cold methanol. A solution of 0.5% crystal violet in 25% methanol was added to the monolayer for 30 min. The dishes were then washed with ddH_2O, and the colonies (at least 50 cells) were counted. The results were expressed as plating efficiency (percentage of colonies formed from the number cells seeded).

Tumor sphere CD133 immunofluorescence

Spheres were cultured as previously described, harvested and then allowed to spontaneously settle in a 50-mL polypropylene conical tube. Excess supernatant was removed. Spheres were dispensed in an 8-well µ-Slide (Ibidi) and allowed to settle, and Matrigel from a 5X Matrigel BME Coating Solution (Trevigen) was added to 0.1X. The cells were fixed in ice-cold methanol for 20 min and permeabilized in 0.5% Triton X-100 containing 0.3% serum for 10 min. Blocking was carried out in Tris-buffered saline (TBS) solution with serum (1:5) for 10 min. The primary antibody anti-CD133 (clone 293C3; Miltenyi Biotec) was diluted in the blocking solution with 0.5% Tween-20, and the spheres were incubated overnight. The cells were washed three times in TBS and incubated with goat anti-mouse Alexa 594 F(ab)2 (in TBS plus 0.5% Tween-20). After three washes in TBS, the nuclei were stained with Hoechst 33342. Images were acquired using a confocal laser scanning microscope (Leica Confocal Microsystem TCS SP5). The images were processed using Leica Application Suite 6000, the brightness and contrast of the acquired images were adjusted, and the figures were generated using Adobe Photoshop 7.0.

Immunoistochemistry

Cerebella of E10, P10 (i.e., 10 d and 18 d of age) and P18 rats (for EGL or lesion analysis) were dissected out and fixed by immersion overnight in 4% PFA in PBS–DEPC. Fixed cerebella were cryoprotected before sectioning in 30% sucrose in PBS–DEPC overnight at 4°C and frozen at −80°C until use. Cerebella were then embedded in Tissue-Tek OCT (Sakura Finetek), and midsagittal sections of 20 µm were cut on a rotary microtome. Primary antibodies used were a mouse monoclonal antibody raised against NeuN (Millipore Bioscience Research Reagents; MAB377; 1:100), a mouse monoclonal antibody against Lamin A/C (clone JOL2; Chemicon International; 1:10). Secondary antibodies used to visualize the antigen was donkey anti-mouse

Cy2-conjugated and Alexa 647-conjugated (Invitrogen). Nuclei were stained with Hoechst 33342. Images of the immunostained sections were obtained by laser-scanning confocal microscopy using a TCS SP5 microscope (Leica Microsystems) and were analyzed by the I.A.S. software (Delta Sistemi).

Western blot analysis

GCs monolayers were washed twice with 1X PBS and then incubated for 1 min in urea buffer (8M urea, 100mM NaH2PO4 and 10mM Tris pH 8), harvested and briefly sonicated. The proteins were run on a pre-cast polyacrylamide NuPAGE 10% Bis-Tris gel (Life Technologies). The resolved proteins were blotted overnight onto nitrocellulose membranes, then blocked in 1X PBS containing 5% non-fat milk for at least 1 h. The blots were incubated with the following primary anti-human antibodies: monoclonal anti-Lamin A/C (clone JOL2; Chemicon International); monoclonal anti-GAPDH (6C5; Millipore). After washing, the membranes were then incubated for 45 min with the secondary donkey anti-mouse or anti-rabbit antibody IRdye800 (LI-COR). After further washing, membranes were then analysed with a Licor Odyssey Infrared Image System in the 800 nm channel. Blot scan resolution was 150 d.p.i.

N-Myc FACS analysis

SH-SY5Y CTR, LMNA-KD cells and TICs were analyzed by indirect immunofluorescence. The cells were harvested, washed in cold 1X PBS and fixed (1x106 cells/ml) in a solution containing cold acetone/methanol (1:4 v/v) in 50% 1X PBS. For each sample, 1x106 cells were incubated with the human monoclonal antibody anti-N-Myc (Santa Cruz) in medium containing 10% FBS and 0.5% Tween 20 for 1 h at room temperature. After washing in PBS, the cells were incubated with FITC-conjugated goat anti-mouse IgG (BD, Pharmingen) in PBS for 50 min. After an additional wash in PBS, the samples were measured using a FACSCalibur cytofluorimeter (Becton Dickinson). Samples incubated with IgG isotype control antibody were used as negative controls, and NB LAN-5 cells were used as a positive control. The analysis was performed using the CellQuest software package. To determine the N-Myc immunofluorescence positivity we used the method of 2% of background.

Side population

To analyze the side population phenotype, LMNA-KD cells were stained according to the protocol of Goodell et al. [35]. Briefly, $5.0x10^6$ cells/ml were suspended in pre-warmed DMEM. Hoechst 33342 (Sigma) was added at a final concentration of 5 µg/ml in the presence or absence of 50 µM verapamil (Sigma), and the cell samples were incubated for 90 min at 37°C with intermittent shaking. After incubation, the cells were washed with ice-cold PBS, resuspended in ice-cold PBS, and analyzed for Hoechst33342 efflux with a FACS Aria II (Becton Dickinson). The Hoechst 33342 dye was excited at 375 nm, which is near-ultraviolet, and the resultant fluorescence was measured at two wavelengths, using 450/40 BP and 670 LP filters for the detection of Hoechst blue and red, respectively. All data were analyzed using the Diva 6.1 Software (Becton Dickinson).

In vivo experiments

Six- to eight-week-old CD-1 male nude (nu/nu) mice weighing 22–24 g were purchased from Charles River Laboratories (Calco, Italy). The procedures involving mouse care were in compliance with the Regina Elena National Cancer Institute animal care guidelines and with international directives (directive 2010/63/EU of the European parliament and council; Guide for the Care and Use of Laboratory Animals, United States National Research Council, 2011). To evaluate the tumorigenic ability of LMNA-KD cells or sphere-derived adherent cells, the mice were injected subcutaneously into the left flank with various concentrations of cells (from $5x10^4$ to $1x10^7$ cells/mouse) in 200 µl of Matrigel (BD Biosciences-Discovery Labware). Each group included five mice. Tumor sizes were measured three times a week in two dimensions using a caliper, and tumor weight was calculated using the following formula: $a \times b^2/2$, where a and b are the long and short diameters of the tumor, respectively.

Histopathological analysis

The engrafted tumors were fixed with 4% phosphate-buffered formalin, and paraffin-embedded sections were stained using hematoxylin and eosin (H&E). The sections were then subjected to morphological analysis.

Total RNA preparation

Total RNA was isolated using a Total RNA purification kit (Norgen Biotek). RNA quantity was determined by measuring absorbance at 260 nm using a NanoDrop UV-VIS spectrophotometer. The quality and integrity of each sample was confirmed using a BioAnalyzer 2100 (Agilent RNA 6000 Nanokit); samples with an RNA Integrity Number (RIN) index lower than 8.0 were discarded.

PCR Array

RNA was reverse transcribed using TaqMan MicroRNA Reverse Transcription kit (Applied Biosystems). cDNA was preamplified using TaqMan PreAmp Master Mix (Applied Biosystems). qRT-PCR was performed with an Applied Biosystem 7900HT thermal cycler using TaqMan human microRNA array (TaqMan Human microRNA Array A #4398977 and B v3.0 #442812; Applied Biosystems) according to manufacturer's instructions. The downstream analysis filtered out miRNAs not detected in both cell lines (293), whereas those specifically expressed either in LAN-5 or in SH-SY5Y were considered and reported as cell line-specific. Data were then normalized calculating the ΔCt value for single miRNA against the average of the specific controls for each card according to manufacturer's instructions. Differential expression analysis was performed according to ΔΔCt method and only RQ $\geq$ 2 fold-change were considered for further analysis. miRNAs clusters were generated through the DIANA web tool mirPath v2.0 using miRBase MIMAT IDs (Release 21) remapped to the newest human genome assembly (GRCh38) to avoid duplicate entries present in the previous release. Uniquely targets reported in TarBase database v7.0 were included in the clustering, predicted targets were not taken into account. False Discovery Rate (FDR) correction was applied to the original p-value and only clusters with corrected p-values < 0.05 were shown.

miRNA Assays

Equal amounts of RNA were reverse transcribed with the TaqMan® MicroRNA Reverse Transcription Kit (Applied Biosystems) according to the manufacturer's instructions, with a custom 1X RT primer pool (hsa-miR-101-3p ID 002253; has-miR-34a ID 000426; U6 snRNA ID 001973). Real time PCR analysis was performed with an Applied Biosystems 7900HT thermal cycler using 20X Individual TaqMan® MicroRNA Assays.

Hsa-miR-101 inhibitor and mimic

SH-SY5Y control and LMNA-KD cells were seeded at a density of $5x10^4$ cells/cm^2. After 24 h, the cells were transfected overnight in the presence of 10% FBS with mirVana miRNA inhibitor, miRNA mimic or the respective negative controls. Lipofectamine RNAiMAX Reagent (Life Technologies) was used as the transfection reagent, according to the manufacturer's instructions. We transfected the has-miR-101 inhibitor (MH11414, Ambion) and the mimic (MC11414, Ambion) at a final concentration of approximately 50 nM. The mirVana miRNA inhibitor and mimic negative control were used at the same final concentration of 50 nM. Samples were harvested at 72 h to perform mRNA expression analysis.

Real-time RT-PCR analysis

RNA (500 ng) was retro-transcribed with High-Capacity cDNA Reverse Transcription Kit (Applied Biosystem) according to the manufacturer‟s instructions. Equal amount of cDNA was then subjected to real time PCR analysis with an Applied Biosystems 7900HT thermal cycler, using the SensiMix SYBR Kit (Bioline) and the following specific primers at a concentration of 200 nM:

Primer	Unigene	Sequence
ABCG2	Hs. 480218	F: TGGCTTAGACTCAAGCACAGC R: TCGTCCCTGCTTAGACATCC
BMI1	Hs.380403	F: TTCTTTGACCAGAACAGATTGG R: GCATCACAGTCATTGCTGCT
CD34	Hs. 374990	F: GCGCTTTGCTTGCTGAGT R: GGGTAGCAGTACCGTTGTTGT
CD44	Hs. 502328	F: GACACCATGGACAAGTTTTGG R: CGGCAGGTTATATTCAAATCG
EDN1	Hs. 511899	F: TGAGAGGAAGAAAAATCAGAAGAAG R: TTTCTCATGGTCTCCGACCT
ENPP2	Hs. 190977	F: GCACATCGAATTAAGAGAGCAG R: GGGGGAGTCTGATAGCACTG
GAPDH	Hs.544577	F: AGCCACATCGCTCAGACA R: GCCCAATACGACCAAATCC
MYCN	Hs.25960	F: CCACAAGGCCCTCAGTACC R: TCCTCTTCATCATCTTCATCATCT
NANOG	Hs.635882	F: AGATGCCTCACACGGAGACT R: TTTGCGACACTCTTCTCTGC
NES	Hs. 527971	F: TGCGGGCTACTGAAAAGTTC R: TGTAGGCCCTGTTTCTCCTG

POU5f	Hs.249184	F: CTTTGAGGCTCTGCAGCTTAG R: GGTTTCTGCTTTGCATATCTCC
PROM-1	Hs.614734	F: TCCACAGAAATTTACCTACATTGG R: CAGCAGAGAGCAGATGACCA
SOX2	Hs.518438	F: TGCTGCCTCTTTAAGACTAGGAC R: CCTGGGGCTCAAACTTCTCT
TBP	Hs.590872	F: GAACATCATGGATCAGAACAACA R: ATAGGGATTCCGGGAGTCAT
VIM	Hs.455493	F: GTTTCCCCTAAACCGCTAGG R: AGCGAGAGTGGCAGAGGA
Gabra6	Rn.29890	F: AATGTCAGTCGGATTCTTGACA R: TGTTTTGACCTCTGTTACAGCAC
Lmna	Rn.44161	F: GAGCAAAGTGCGTGAGGAGT R: TCCCCCTCCTTCTTGGTATT
Prom1	Rn.144589	F: GCATTCTCAGACCTGGACAGT R: TGGGTTTTAGTTGGCCCTTT
Nes	Rn.9701	F: CCCTTAGTCTGGAGGTGGCTA R: GGTGTCTGCAACCGAGAGTT
Tbp	Rn.22712	F: CCCACCAGCAGTTCAGTAGC R: CAATTCTGGGTTTGATCATTCTG
Tubb3	Rn.43958	F: CAGAGCCATTCTGGTGGAC R: GCCAGCACCACTCTGACC
Zic2	Rn.64359	F: TCAACACACCAACCCATAGC R: AAAAATACATTCACAAGCGTTGG

Each experiment was performed in triplicate. The expression data were normalized using the Ct values of GAPDH and TBP.

Statistical analysis

Student's t test (unpaired, two-tailed) was used for statistical comparison of different tumor weights and between two groups. If there were more than two groups, we used the one-way ANOVA test.

4 RESULTS

Abundance of LMNA in NB tumors is inversely correlated with that of MYCN gene

We analyzed the expression levels of the LMNA and MYCN genes in 23 NB biopsies obtained from the Department of Pediatrics and Infantile Neuropsychiatry of Sapienza University. The tumors were classified according to the International Neuroblastoma Pathology Classification (INPC) and staged as stages 1 to 4. Nine of 23 cases showed amplification of MYCN DNA. The expression levels of the two genes significantly inversely correlated (p=0.01), independently of the DNA amplification of MYCN, in 21 out of the 23 cases analyzed; i.e., as LMNA increased, MYCN gene expression decreased (Fig. 1).

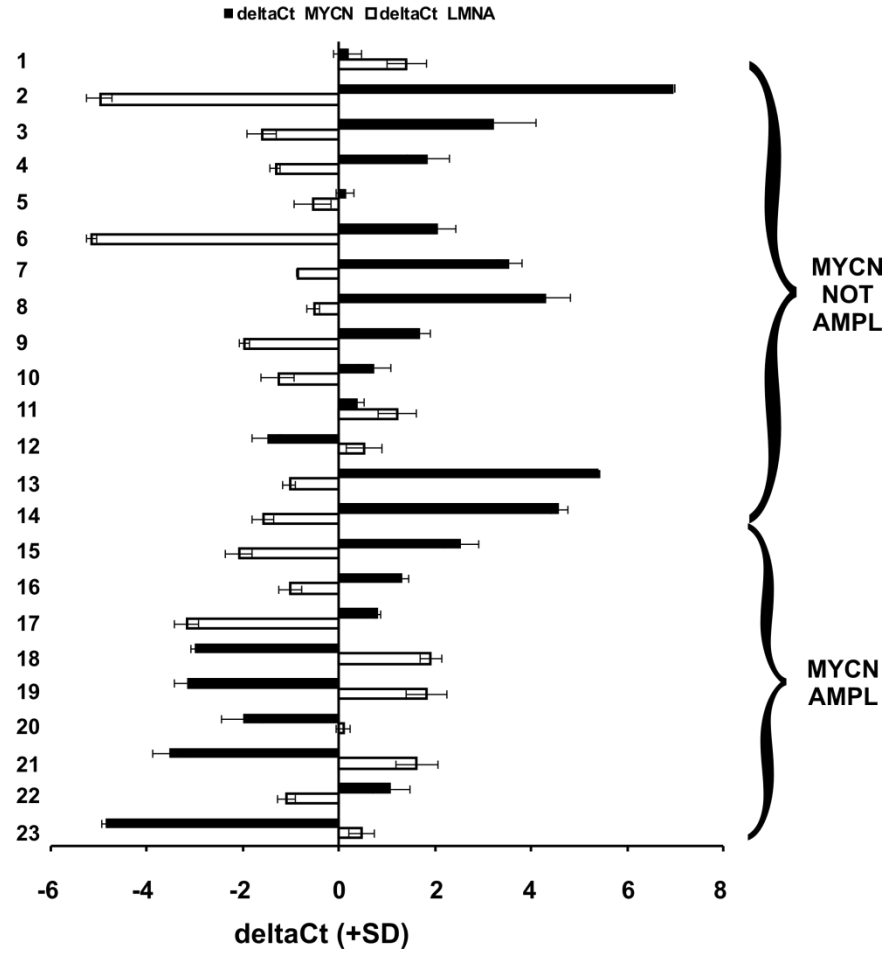

Figure 1. The expression of LMNA and MYCN are inversely correlated in NB human biopsies.
qRT-PCR analysis of the LMNA (white) and MYCN (black) genes in 23 NB human biopsies. Data (means+SD [n=3]) are reported as the deltaCt values normalized against the endogenous control. The deltaCt values are inversely correlated with the amount of the gene present in the sample. Statistical significance: **$p \leq 0.01$.

We decided to study this inverse relationship between LMNA and MYCN gene in an *in vitro* experimental model of NB. We choose the SH-SY5Y and LAN-5 cell lines, which express only LMNA or MYCN gene encoding proteins, respectively (data not shown). In particular, since Lamin A/C has been demonstrated to play an epigenetic role in regulating gene expression and miRNAs can be targeted by MYCN, we hypothesized a possible reciprocal regulation between the two genes mediated by miRNAs.

We performed a miRNA expression profiling of LAN5 and SH-SY5Y cells using TaqMan Human MicroRNA Arrays. A total of 768 miRNAs, present in the array, were analyzed in each cell line. The distribution of the expressed miRNAs is shown in a Venn diagram where a total of 417 (66 specific and 351 common) and of 395 (44 specific and 351 common) miRNAs were found expressed in LAN-5 and SH-SY5Y cells, respectively (Fig. 2A). We found 359 and 337 miRNAs not expressed in SH-SY5Y and LAN-5 cells, respectively (293 not expressed at all in both cell lines). We identified a set of 202 out of the 351 common miRNAs differentially expressed at least 2-fold change between the two cell lines (99 in the LAN-5 and 103 in the SH-SY5Y cells); whereas 149 miRNAs were filtered out by the threshold applied. A scatter plot analysis shows the correlation between miRNA expression values (Ct) in LAN-5 and SH-SY5Y cell lines (Fig. 2B). Grey dots distributed along the bisector line represent miRNAs similarly expressed in the two lines (n=149). While, red or green dots correspond to miRNAs with high expression in the LAN-5 (n=165) and SH-SY5Y (n=147), respectively.

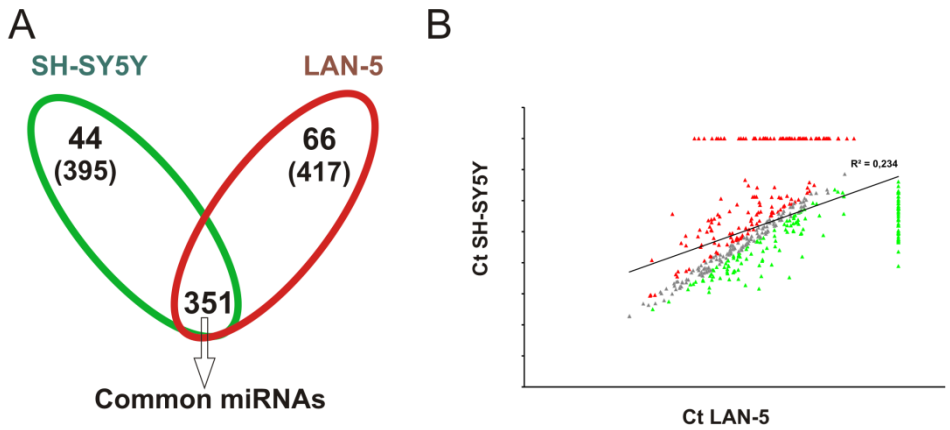

Figure 2. Functional analysis of miRNA target genes in LAN-5 and SH-SY5Y cell lines.
(**A**) Venn diagram of expressed miRNAs in SH-SY5Y and LAN-5 cells. The number in parenthesis represents the total miRNAs expressed in each line. (**B**) Scatter plot of the miRNA Ct values normalized against endogenous controls in SH-SY5Y and LAN-cells. Grey dots represent unchanged miRNAs between the two cell lines; green dots are the SH-SY5Y miRNAs; red dots represent LAN-5 miRNAs.

Considering the specifically and the differentially expressed miRNAs we performed a functional analysis using the DIANA-mirPath 2.0 tool, and in particular the software TarBase which uniquely clusters those miRNAs whose targets are experimentally validated (Vlachos et al., 2014). We filtered the clusters obtained based on their significance (FDR corrected $p < 0.05$). As to be expected, target genes resulted grouped into functional categories associated with cancer phenotype. The most modulated miRNAs in both cell lines belong to pathways involved in the regulation of cell proliferation, apoptosis, and response to treatment: "p53 signaling pathway", "cell cycle", "pathways in cancer", "PI3K-Akt signaling pathway", "transcriptional misregulation in cancer". These pathways are consistent with the inherent phenotypic characteristics of the two cell lines and correlate to their different capacity to proliferate, to undergo apoptosis, to migrate and invade (Appendix). Since a single miRNA can inhibit several target mRNAs and multiple miRNAs can target a single mRNA in a combinatorial fashion, to identify more accurately the differences between the miRNome profiles of these two NB cell lines, we intersected the target genes derived from the two cell lines in order to identify the identical genes which were then removed from the analysis. In Table 1 are reported target genes, and relative miRNAs, identified only in SH-SY5Y or LAN-5 cells after removing the identical genes.

Table 1. Target genes and relative miRNAs specifically expressed only in LAN-5 cells (red) or SH-SY5Y (green)

KEGGterm	Count	PValue	Genes					Count	miRNA|TarBase	
hsa04110:Cell cycle	6	4.05E-32	BUB1B PRKDC	ORC6	PKMYT1	SMAD3	SMAD2	2	miR-155-5p	miR-193b-3p
hsa05200:Pathways in cancer	21	1.12E-08	RAC2 CDH1 HSP90AB1 CTNNA1 BAX	RAD51 FN1 CASP9 JUP	TCF7L1 SUFU MAX SMAD3	NFKB2 RHOA NKX3-1 FGF2	SMAD2 RAC2 FGF7 CDK2	5	miR-155-5p miR-193b-3p miR-504	miR-378a-5p miR-200c-3p
hsa04115:p53 signaling pathway	2	1.35E-05	BAX	RCHY1				2	miR-504	miR-19a-3p
hsa04110:PI3K-Akt signaling pathway	15	8.07E-03	EIF4E2 ITGB4 THBS1	FGF2 ITGB5 YWHAZ	FGF7 RHEB NFKB1	FLT1 PKN2 PCK2	GNB4 PRKCZ PDK1	2	miR-155-5p	miR-19a-3p
hsa05202:Transcriptional misregulation in cancer	2	4.32E-02	CD40	BCL2L1				2	miR-486-5p	miR-491-5p

KEGGterm	Count	PValue	Genes						Count	miRNA|TarBase		
hsa04115:p53 signaling pathway	22	1.08E-29	APAF1	CASP8	SESN1	MDM4	CDKN2A	TP73	18	miR-101-3p	miR-26b-5p	miR-21-5p
			ATM	CCND3	SFN	PIDD1	DDB2	ZMAT3		miR-424-5p	miR-93-5p	miR-193a-5p
			BID	CCNE1	THBS1	RFWD2	EI24	GADD45A		miR-34a-5p	miR-24-3p	miR-374a-5p
			CASP3	CCNG2	TP53I3	SERPINB5						
hsa05200:Pathways in cancer	51	5.47E-24	APPL1	CCNE1	FGF1	ITGA6	MMP2	TP53	36	miR-214-3p	let-7c	miR-222-3p
			AR	CHUK	FGFR1	JUN	MMP9	BMP2		let-7d-5p	miR-21-5p	miR-25-3p
			AXIN2	CRKL	FZD4	LAMC2	NFKBIA	ERBB2		miR-424-5p	miR-363-3p	miR-24-3p
			BID	DAPK1	HDAC1	MAP2K1	NRAS	IKBKB		miR-146b-3p	miR-93-5p	miR-503
			PLD1	STAT1	VHL	RALA	TCF4	MMP1		miR-449a	miR-34a-5p	miR-26a-5p
			PTK2	STAT5A	WNT1	RALB	TFG	PIK3R1		let-7f-5p	miR-223-3p	miR-28-5p
			RB1	TGFB2	RUNX1	TGFBR1	SKP2	PDGFB		miR-27a-3p	miR-29b-3p	miR-374a-5p
			BIRC3	DVL2	HSP90AA1	MAPK1	PDGFA	MAPK9		miR-769-5p	miR-28-5p	miR-361-5p
			BIRC5	E2F3	IGF1R					miR-221-3p	miR-199b-5p	miR-361-5p
hsa04110:Cell cycle	17	6.56E-21	ANAPC13	ATM	CCND3	CCNE1	CDC14A	GADD45A	14	miR-424-5p	miR-34a-5p	let7d-5p
			MDM2	ORC4	SFN	SKP2	TP53	HDAC1		miR-374a-5p	let-7c	miR-25-3p
			CDC23	CDC25C	E2F3	E2F5	EP300			mirR-503	mir-769-5p	
hsa04110:PI3K-Akt signaling pathway	32	1.02E-07	PDGFA	MAP2K2	IGF1R	FGFR1	COL3A1	CASP9	26	let-7c	miR-449a	miR-100-5p
			PDGFB	MDM2	IKBKB	FGFR3	COL4A1	CCNE1		let-7f-5p	miR-503	miR-424-5p
			PDGFC	MYB	INSR	GNG5	COL5A3	CDC37		miR-7-5p	miR-146b-3p	miR-181c-5p
			PIK3CB	NRAS	IRS1	HSP90AA1	EIF4E	CHUK		miR-222-3p	let-7d-5p	miR-29b-3p
			PPP2R1B	PAK1	MAP2K1	IFNB1	FGF1	COL1A1		miR-26a-5p	miR-34b-5p	
			PRKAA1	RAF1								
hsa05202:Transcriptional misregulation in cancer	39	3.14E-03	TGFBR2	PDGFB	MEIS1	Il6	HIST2H3C	HIST1H3H	19	miR-34a-5p	miR-223-3p	miR-363-3p
			TP53	RUNX1	MYC	KLF3	HIST3H3	HIST1H3I		miR-146b-3p	miR-93-5p	miR-25-3p
			ZEB1	SMAD1	MYCN	LMO2	HOXA9	HIST1H3J		miR-27a-3p	miR-26a-5p	miR-101-3p
			SP1	PAX3	MEF2C	IGF1R	HIST2H3A	HIST1H3E		miR-28-5p		
			HIST1H3C	H3F3B	CEBPB	BIRC3	CDKN2C	BAIAP3				
			HDAC1	FOXO1	CCND2	ATM	HIST1H3B	H3F3A				
			HIST1H3A	GOLPH3	CDKN1B							

The gene ontology performed using the DAVID tool on this subset of target genes revealed that the most relevant enriched functional categories identified in SH-SY5Y cells were associated to cell migration, locomotion and cell proliferation (Fig. 2C and Table 2). This indicates that SH-SY5Y cells, which express LMNA gene, have a reduced ability to migrate, to proliferate and hence to be aggressive. Whereas, the LAN-5 cells, which instead express MYCN gene, showed an enrichment in functional categories associated with regulation of differentiation and cell proliferation suggesting that these cells are less prone to differentiate and might show a stem-like phenotype with respect to SH-SY5Y cells (Fig. 2C and Table 2). On the basis of these results, we hypothesize that the mutual expression of MYCN and LMNA genes could address NB cells to a stem-like or a differentiating phenotype, respectively.

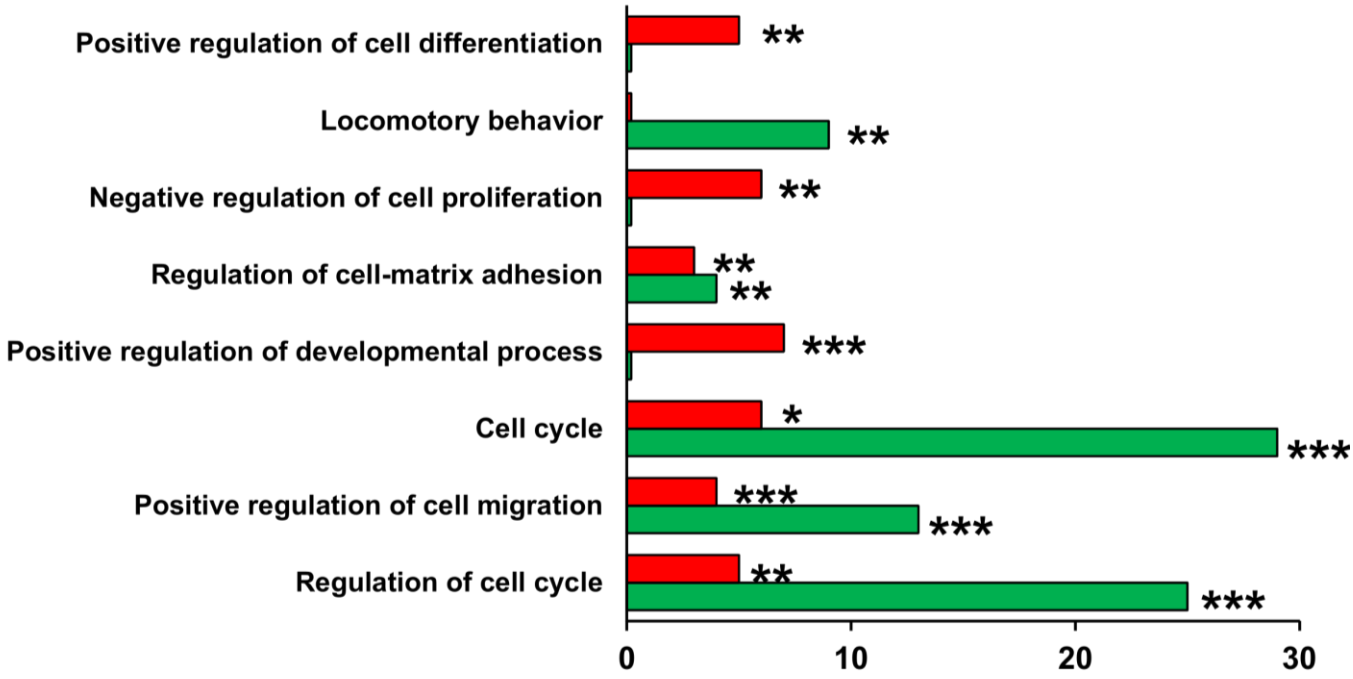

Figure 3. Gene ontology by DAVID.
In the histogram are reported the number of target genes belonging to the indicated functional categories. Red bar, LAN-5 cells; green bar, SH-SY5y cells. Statistical significance: *p≤0.05, **p≤0.01, ***p≤0.001.

Table 2. Gene Ontology analysis on the target genes specifically expressed only in LAN-5 (red) or SH-SY5Y (green)

GOTERM	Pvalue	Count	Genes
GO:0051094~positive regulation of developmental process	9,707E-05	7	BAX RHOA SMAD3 NFKB1 SMAD2 THBS1 FGF2
GO:0001952~regulation of cell-matrix adhesion	0,002	3	PRKCZ SMAD3 THBS1
GO:0008285~negative regulation of cell proliferation	0,003	6	BAX NKX3-1 SMAD3 SMAD2 THBS1 FGF2
GO:0045597~positive regulation of cell differentiation	0,004	5	RHOA SMAD3 NFKB1 SMAD2 FGF2

GOTERM	Pvalue	Count	Target Genes
GO:0051726~regulation of cell cycle	4,84E-16	25	STAT5A SFN CCNG2 CDC37 TGFB2 CASP3 CDKN2A CDKN2C INSR MYC BMP2 TP53 SKP2 CDC23 BIRC5 RB1 CDC25C ATM CDKN1B HDAC1 CCND3 CCND2 JUN MDM2 GADD45A
GO:0030335~positive regulation of cell migration	1,21E-11	13	IL6 PLD1 PDGFB MAP2K1 PDGFA MMP9 IRS1 TGFB2 IGF1R MAPK1 THBS1 INSR PIK3R1
GO:0007049~cell cycle	5,21E-11	29	E2F3 CDC14A ANAPC13 SESN1 CCNG2 TGFB2 CCNE1 CDKN2A CDKN2C THBS1 MYC, MAP2K1 TP53 SKP2 CDC23 BIRC5 RB1, CDC25C APPL1 ATM TP73 MAPK1 CDKN1B EP300 CCND3 CCND2 MDM2 MDM4 GADD45A
GO:0001952~regulation of cell-matrix adhesion	0,002	4	CDKN2A PIK3CB THBS1 PIK3R1
GO:0007626~locomotory behavior	0,003	9	MAPK1 PLD1 IL6 MAP2K1 PDGFB PDGFA PIK3CB RALA TGFB2

LMNA gene knock-down induces a stem-like phenotype in SH-SY5Y cells

We used as experimental model the SH-SY5Y cells in which we previously inhibited differentiation by LMNA knock-down (LMNA-KD; Maresca et al., 2012). First, we analyzed the expression of some stemness-related markers such as NANOG, SOX2, POU5f, PROM-1, CD34 and ABCG2, by qPCR (Fig. 4A). All of these genes were overexpressed in LMNA-KD cells, indicating that lack of the LMNA gene could be associated with a more immature cell phenotype. The activity of ABCG2, which is a member of the ATP-binding cassette (ABC) membrane transporters and is active in many types of stem cells, was also verified evaluating by FACS analysis the exclusion of the fluorescent supravital dye Hoechst 33342 out of the cells. The cells able to pump outside the dye is concentrated in a tailing population exhibiting dim fluorescence relative to the majority of cells with bright fluorescence and they represent the so called "side population", known to correlate with a stem-like phenotype. Indeed, LMNA-KD cells show the presence of a side population identified by a Hoechst 33342 low-staining fraction (approximately 5%; Fig. 4B). As control to confirm dye efflux and the probable presence of stem-like cells we inhibited the ABCG2 pump by verapamil. Consistently, verapamil treatment led to depletion of this side population in LMNA-KD cells. By contrast, control cells presented the same cytofluorimetric profile in both the presence and absence of verapamil.

We then investigated the ability to form spheres by LMNA-KD cells in the appropriate culture conditions. As a positive control, we used human NB LAN-5 cells, known to form spheres [3]. Similarly to LAN-5 cells, LMNA-KD cells formed secondary spheres in serum-free medium (Fig. 4C). By contrast, control cells did not show any significant capacity to form secondary spheres. We carried out immunofluorescence experiments on the spheres to detect the expression of a well-known stemness marker, CD133. LMNA-KD secondary spheres were positive for the CD133 marker, detected on the membrane surface (Fig. 4D).

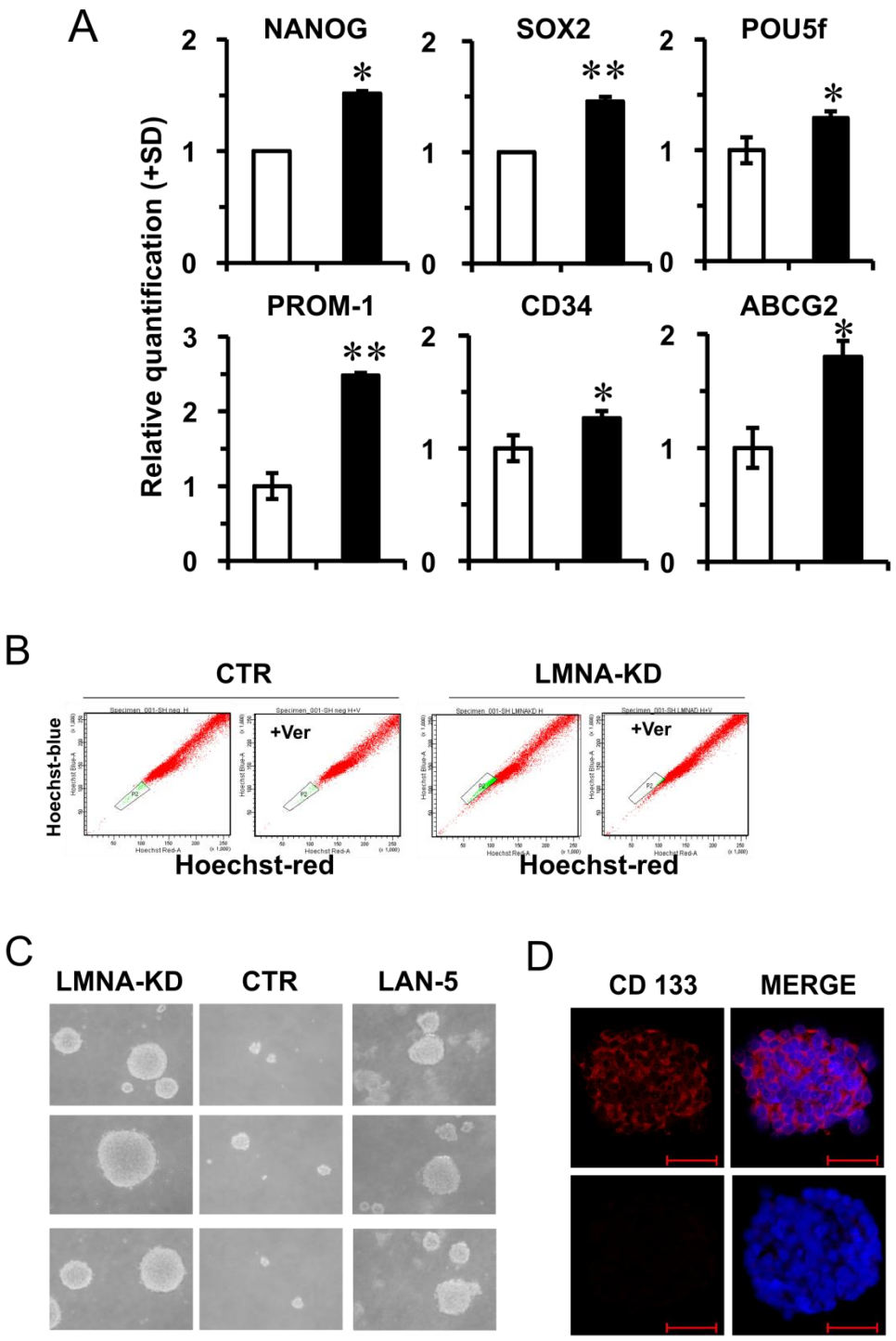

Figure 4. SH-SY5Y LMNA-KD cells acquire stemness characteristics.
(**A**) qRT-PCR analysis of the indicated genes in control (CTR; white) and LMNA-KD (black) cells. The data are reported as the level of mRNA relative to the number of control cells and are the means+SD (n=5). Statistical significance: *p≤0.05, **p≤0.01. (**B**) flow cytometric analysis of side population after staining with Hoechst 33342 in the absence or presence of verapamil to inhibit the functionality of the membrane ABCG2 efflux pump. (**C**) tumor sphere assay of LMNA-KD cells compared to control and LAN-5 cells; phase contrast micrographs of the secondary spheres, magnification 200X. (**D**) representative confocal images of the secondary tumor spheres. CD133 immunostaining (red) and nuclear staining (blue). Scale bar: 50 µm.

LMNA-KD sphere-derived adherent cells maintain stemness characteristics and acquire a more aggressive phenotype

Spheres formed from LMNA-KD cells were cultured in adherent conditions for several passages. Sphere-derived adherent cells grew as discrete groups of differently sized cells whereas the LMNA-KD cell monolayer showed a dispersed pattern, with growing cells being mainly isolated (Fig. 5)

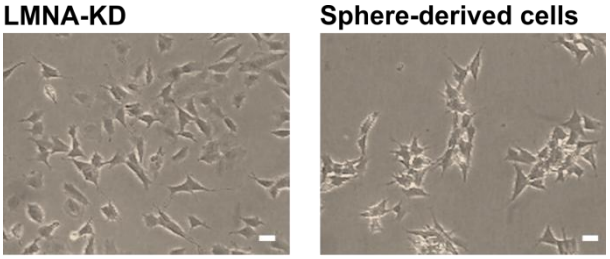

Figure 5. Phase contrast micrograph of LMNA-KD and sphere-derived adherent cells. Scale bar: 10µ.

We verified the expression of MYCN mRNA levels which significantly increased in LMNA-KD cells and in sphere-derived adherent cells (approximately 2-fold) compared with CTR cells thus confirming our hypothesis (Fig. 6A, left panel). The increased MYCN expression was associated with the down-regulation of the NDRG1 and NDRG2 genes in LMNA-KD cells and in sphere-derived adherent cells (Fig. 6A, right panel). An increase in the N-Myc protein accompanied the increase in MYCN gene expression in LMNA-KD cells and sphere-derived adherent cells, as evaluated by FACS analysis (approximately 40 and 65%, respectively; Fig. 6B). We characterized the LMNA–KD sphere-derived adherent cells to evaluate the mRNA expression levels of self-renewal genes compared to those in the LMNA-KD cell line. The stemness marker genes maintained their expression or were further up-regulated in LMNA-KD sphere-derived adherent cells (Fig. 6C). In particular, we observed a strong up-regulation of the stemness network of the transcription factor genes NANOG, POU5f and SOX2 and of the drug resistance-related gene ABCG2. In addition, sphere-derived adherent cells maintained their self-renewal ability, as they were still able to form cell spheres in non-adherent culture conditions.

Sphere-derived adherent cells appeared to acquire a more aggressive phenotype than LMNA-KD cells (Fig. 6D). The ENPP2 metastasis-associated gene showed a 4-fold increase with respect to LMNA-KD cells. In addition, the EDN1 and CD44 genes, known to be involved in cell adhesion functions, significantly decreased in the sphere-derived adherent cell line.

Mainly, these data strongly suggest that LMNA–KD sphere-derived adherent cells possess self-renewal and tumor progression characteristics that are peculiar of a putative population of tumor-initiating cells (TIC-like cells).

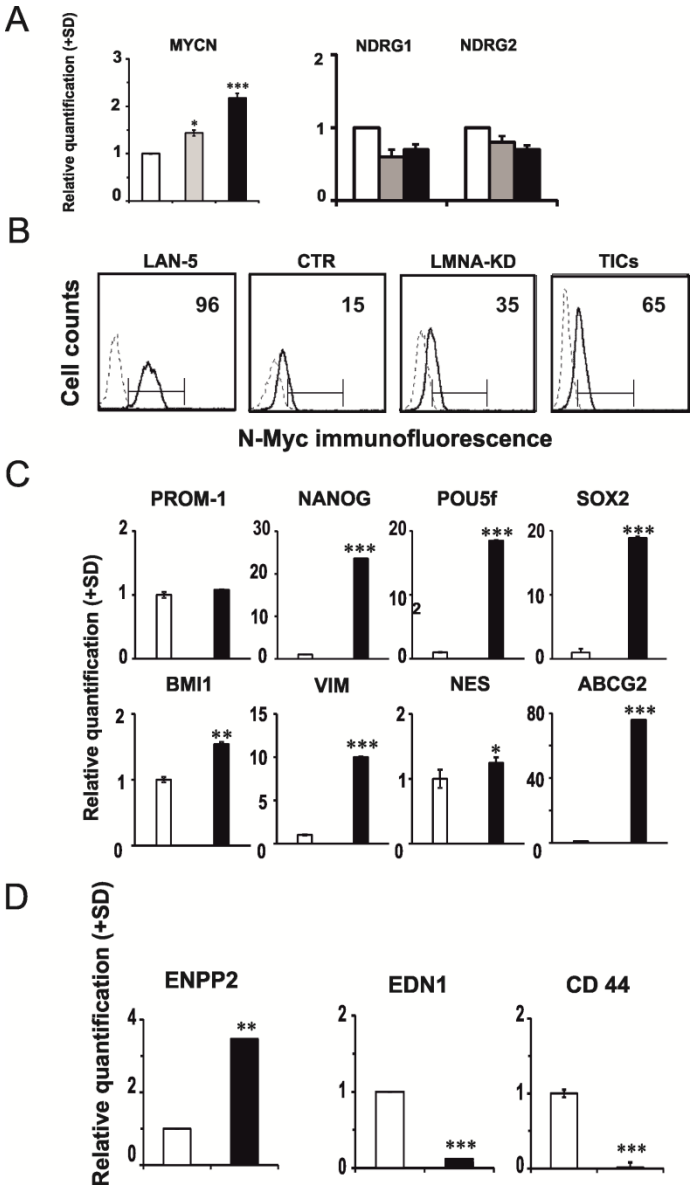

Figure 6. LMNA–KD sphere-derived adherent cells possess self-renewal and tumor progression characteristics. (**A**) RT-qPCR analysis of MYCN mRNA levels (right panel) and of NDRG1 and NDRG2 mRNA levels (left panel) in CTR cells (white), LMNA-KD cells (grey) and LMNA–KD sphere-derived adherent cells (black). The data are reported as the level of mRNA relative to CTR cells and are the means+SD (n=5). Statistical significance: * $p \leq 0.05$ ** $p \leq 0.01$, *** $p \leq 0.001$. (**B**) FACS analysis of N-Myc expression in control and LMNA-KD cells. LAN-5 cells were used as a positive control. The number reported in each histogram represents the percent positivity. (**C**) RT-qPCR analysis of the indicated genes in LMNA-KD cells and the sphere-derived adherent cell line. The data are reported as the level of mRNA relative to LMNA-KD cells and are the means+SD (n=5). Statistical significance: *$p \leq 0.05$, **$p \leq 0.01$, ***$p \leq 0.001$. (**D**) relative expression of tumor aggressiveness-related genes in the sphere-derived adherent line vs LMNA-KD. The data are reported as the level of mRNA relative to LMNA-KD cells and are the means+SD (n=5). Statistical significance: **$p \leq 0.01$, ***$p \leq 0.001$.

The LMNA-KD sphere-derived adherent cell line is able to initiate tumors *in vivo*

We performed a limiting dilution assay in LMNA-KD sphere-derived adherent cells (namely TIC-like cells in this paper) to determine the minimum cell dilution capable of forming colonies *in vitro*. While TIC-like cells maintained colony forming ability at very low dilution (down to 16 cells), LMNA-KD cells did not form colonies at such dilution (Fig. 7A).

On this basis, we compared the *in vivo* growth of the two cell lines using an *in vivo* limiting dilution assay. Immunosuppressed mice were injected subcutaneously with different number of LMNA-KD and TIC-like cells (from $5x10^4$ to $1x10^7$). No differences in terms of tumor appearance and tumor growth were evident injecting from $2.5x10^5$ to $1x10^7$ TIC-like and LMNA-KD cells (data not shown). While, at lower number, TIC-like cells exhibited a higher growth rate than LMNA-KD cells (Fig. 7B); this was evident when mice were injected with 10^5 cells (left panel), but a more marked difference between TIC-like and LMNA-KD cells was found in terms of tumor mass when $5x10^4$ cells were injected per mouse (right panel). In fact, a significant increase in the weight of the TIC-like-derived tumors compared to the LMNA-KD-derived tumors (an almost doubling) was observed as the maximum effect (on day 14 after tumor cell injection) ($P=0.003$).

The histopathological pattern of these tumors, analyzed on day 27 of tumor growth, showed small cells with round to oval shapes, deeply stained nuclei and poorly defined cytoplasmic outlines. Unlike LMNA-KD-derived tumors, TIC-derived tumors were mainly microscopically characterized by a nodular pattern of growth. Small aggregates with mostly hyperchromatic nuclei were defined by the presence of fibrous septa. We also observed hypercellularity and overlapping nuclei occasionally exhibiting small nucleoli in TIC-derived tumors. These findings further demonstrate the more malignant phenotype of TIC tumors (Fig. 7C).

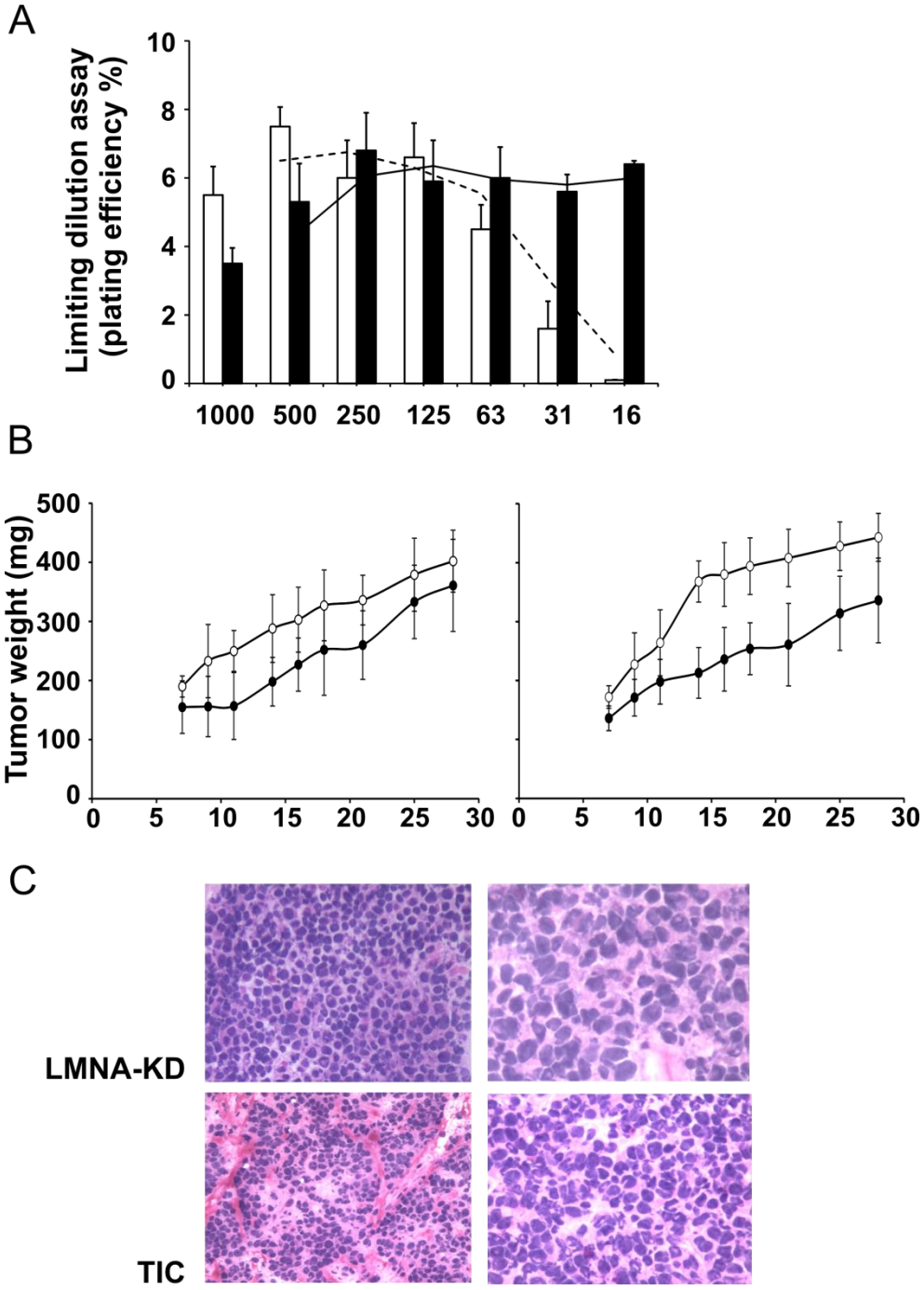

Figure 7. The LMNA-KD sphere-derived adherent cell line is able to initiate tumor growth *in vivo*.
(**A**) *in vitro* plating efficiency (%PE) in LMNA-KD (white) and sphere-derived adherent (black) cells at different cell dilutions. (**B**) LMNA-KD (•) or sphere-derived adherent (○) cells were injected subcutaneously into the flanks of immunosuppressed mice at 10^5 (left panel) or $5x10^4$ (right panel) cells/mouse in 200 µl of Matrigel. When a tumor mass was evident, the tumor sizes were measured, and the tumor weight was calculated using the following formula: $a \times b^2/2$, where a and b are the long and short diameters of the tumor, respectively. The mean±SD tumor weights are reported. (**C**) histopathological examination of tumor biopsies from LMNA-KD cells and TICs after 27 days of tumor growth. Images shown are at 20X (left panels) and 40X (right panels) magnification.

LMNA-KD sphere-derived adherent cells maintain stemness characteristics and acquire a more aggressive phenotype.

From a more accurately analysis of the table 1 we found that MYCN gene appeared as one of the miRNA target in the SH-SY5Y cells, whereas LMNA did not emerge as a miRNA-regulated gene in the LAN-5 cells, thus indicating that the absence of MYCN expression in SH-SY5Y cell line might be the results of miRNA regulation. Since miR-101is a specific miRNA known to target MYCN gene, we inhibited miR-101 in SH-SY5Y control cells to modulate MYCN expression. As control, we overexpressed miR-101 in LMNA-KD cells in order to verify the effect on MYCN gene expression. As expected, the analysis of the intrinsic expression of miR-101 in both cell lines, revealed miR-101 less expressed in LMNA-KD cells by 50% compared to SH-SY5Y control cells (Fig. 8A).

Transfection of SH-SY5Y control cells with the miR-101 inhibitor decreased the expression levels of miR-101 by approximately 50% (Fig. 8B, left panel). Transfection of LMNA-KD cells with the miR-101 mimic resulted in approximately 90-fold increased expression of miR-101 (Fig. 8B, right panel)The analysis of the MYCN transcripts resulted significantly decreased or increased after transduction of miR-101 inhibitor or mimic, respectively (Fig. 8C). We then analyzed the mRNA levels of genes involved in some of the MYCN-regulated pathways such as stemness and aggressiveness. The expression of the same genes up-regulated in SH-SY5Y control cells after the inhibition of miR-101, decreased in LMNA-KD cells after the overexpression of miR-101. Consistently, after inhibiting miR-101, SH-SY5Y control cells showed down-regulation of the tumor suppressor EDN1 and CD44 genes, and increased expression of the tumor progression ENPP2 gene with respect to LMNA-KD cells transfected with the miR-101 mimic (Fig. 8C).

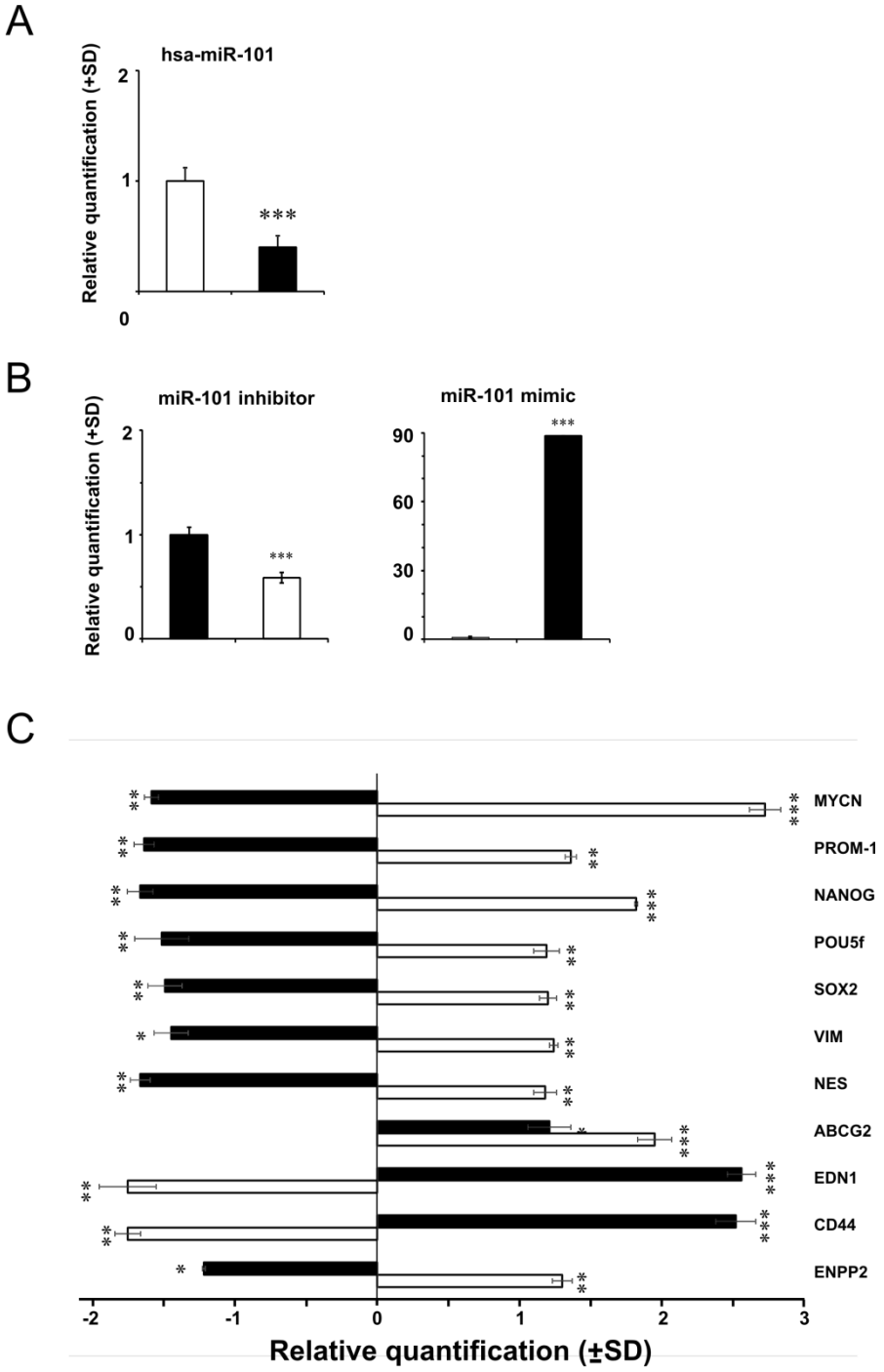

Figure 8. Modulation of hsa-miR-101 modifies the expression of MYCN gene and in turn of stemness and cancer-related genes.

(**A**) TaqMan MicroRNA Assay with hsa-miR-101 in CTR cells (white) and LMNA-KD cells (black). The data are reported as the level of mature miRNA relative to CTR cells and are the means+SD (n=5). Statistical significance: *** $p \leq 0.001$. (**B**) TaqMan MicroRNA Assay, with the hsa-miR-101 levels in CTR cells transfected with the inhibitor (white, left panel) or in LMNA-KD cells transfected with the mimic (black, right panel). The data are reported as the level of mature miRNA compared to each relative negative control and are the means+SD (n=5). Statistical significance: *** $p \leq 0.001$ (**C**) qRT-PCR analysis of the indicated genes in hsa-miR-101 mimic-transfected LMNA-KD cells (black) and hsa-miR-101 inhibitor-transfected CTR cells (white). The data are reported as the level of mRNA compared to each relative negative control and are the means+SD (n=5). Statistical significance: *$p \leq 0.05$, **$p \leq 0.01$, ***$p \leq 0.001$

Lamin C increased during GCs maturation processes both *in vivo* and *in vitro*

Since Lamin A/C has been proposed to be essential during neuron differentiation, we analyzed its expression during cerebellum granule cell (GC) development; an excellent experimental model for molecular and cell biological studies of neuronal development.

Recent studies have uncovered a peculiar pattern of nuclear lamin expression in the brain. Lamin C transcripts are present at high levels in the brain, but Lamin A expression levels are very low due to regulation by miR-9 of their transcripts of the prelamin A level (Young et al., 2014).

Our first observation was the up-regulation of Lamin C expression in GCs *in vivo*. Figure 1A show representative immunofluorescent images of rat cerebellum tissue in which Lamin C increased during GCs development from embryonic stage (E10) to postnatal stage (P18). Lamin C increment was also accompanied by the up-regulation of the well known neuronal marker NeuN (Fig. 9A).

Once GCs were dissociated from rat cerebellum tissue, we confirmed the increase of Lamin C also in primary cell cultures: in Fig. 1B we reported the up-regulation of this protein during GCs maturation at 2, 5 and 8 day *in vitro* (DIV) (Fig. 9B) with the consistent increase of correspondent mRNA (Fig. 9C).

GCs maturation and differentiation *in vitro* were confirmed by the increment of the differentiation-related genes such as Tubb3, expressed during neurite outgrowth, Zic2, member of the zinc finger proteins and specifically expressed in the cerebellum during differentiation, and Gabra6, GABAA receptor alpha6 subunit gene expression, which marks cerebellar granule cell maturation, and the subsequent decrement of the stemness-related genes, Prom-1 and Nes.

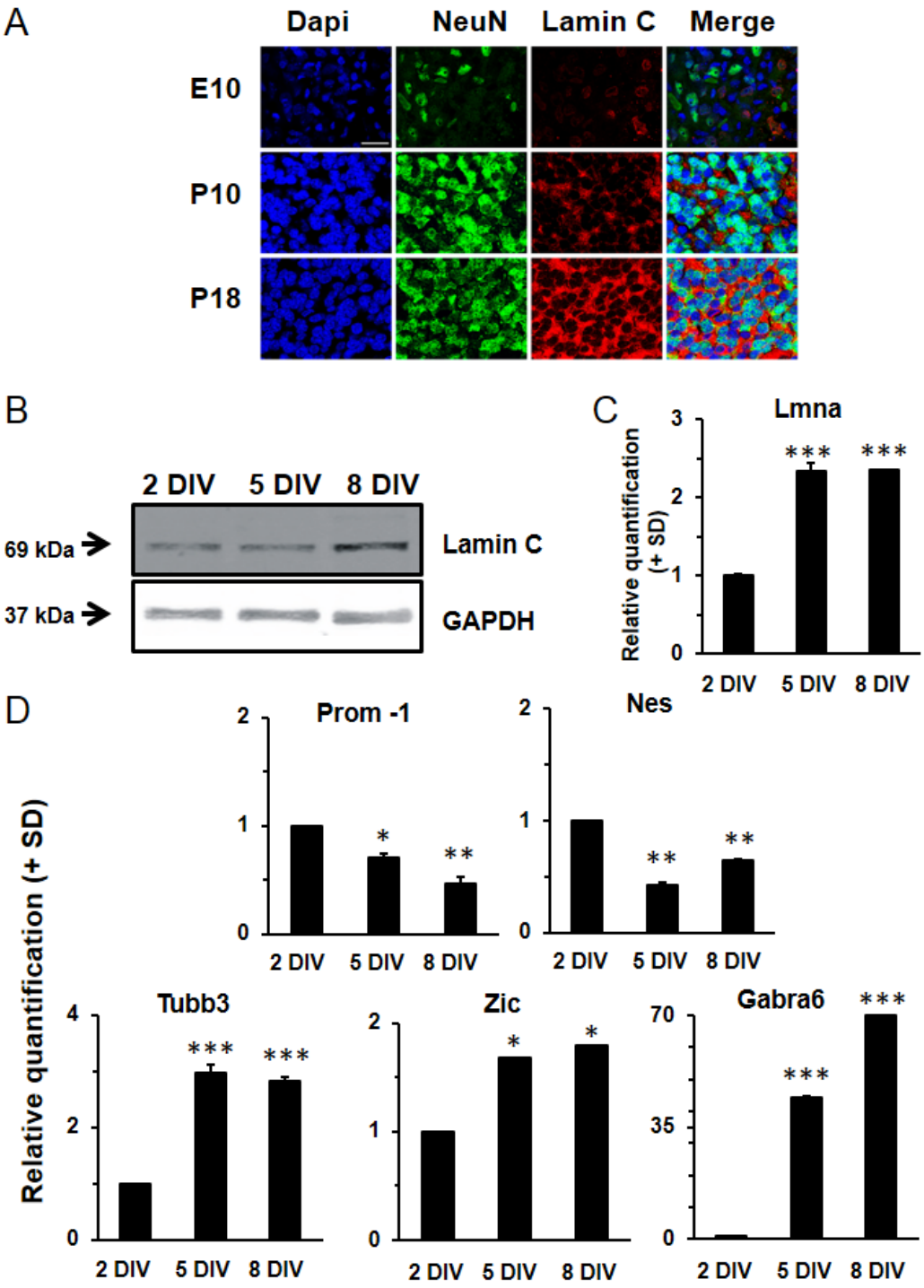

Figure 9. Lamin C increases during GCs maturation.
(**A**) Representative confocal images of rat cerebellar slices of embryonic (E10) and post-natal (P10, P18) days. Lamin C immunostaining (red), Neuronal Nuclei (NeuN) immunostaining (green) and nuclei staining (blue). Scale bar: 40 microns. (**B**) Representative blots of the Lamin C in GCs during 2 DIV, 5 DIV and 8 DIV. GAPDH was used to normalized protein loading. The experiments was repeated three times showing similar results. (**C**) RT-qPCR analysis of LMNA gene in GCs. The data are reported as the level of mRNA relative to 2 DIV GCs and are the mean+SD (n=5). Statistical significance: ***p≤0.001. (**D**) Levels of the indicated mRNA in GCs during 2 DIV, 5 DIV and 8 DIV. The data are reported as the level of mRNA relative to 2 DIV and are the mean + SD (n = 3). Statistical significance, *p≤0.05; **p≤0.01; ***p≤0.001.

Lamin C silencing prevents the complete maturation of GCs

To investigate the role of Lamin C in GCs maturation, we silenced LMNA gene in this model using a vector expressing an artificial miRNA that directly targets LMNA mRNA (Maresca et al., 2012). The LMNA silenced GCs show a reduction in Lamin C expression of about 50% compared to control (CTR) cells infected with a control vector.

We evaluated the expression of neuronal and stemness markers in LMNA-KD GCs and observed the up-regulation of Prom-1 and Nes genes and the down-regulation of Tubb3, Zic and Gabra6 genes (Fig. 10A). All these data taken together suggest that Lamin C may have a role in GC maturation processes.

The primary cultures of GCs have a short life, in fact as their maturation progresses they become gradually more and more vulnerable to the effect of glutamate, and after eight days of culture they reach their full maturity and die by necrosis. For that reason, we analyzed cell survival in LMNA-KD GCs compared to CTR GCs- after glutamate stimulation. Fig. 10B show how LMNA-KD GCs presented a higher percentage of surviving cells after glutamate treatment than CTR GCs-. Thus, Lamin C knock down seems to prevent glutamate-mediated spontaneous neuronal death and, as consequence, the complete maturation of GCs.

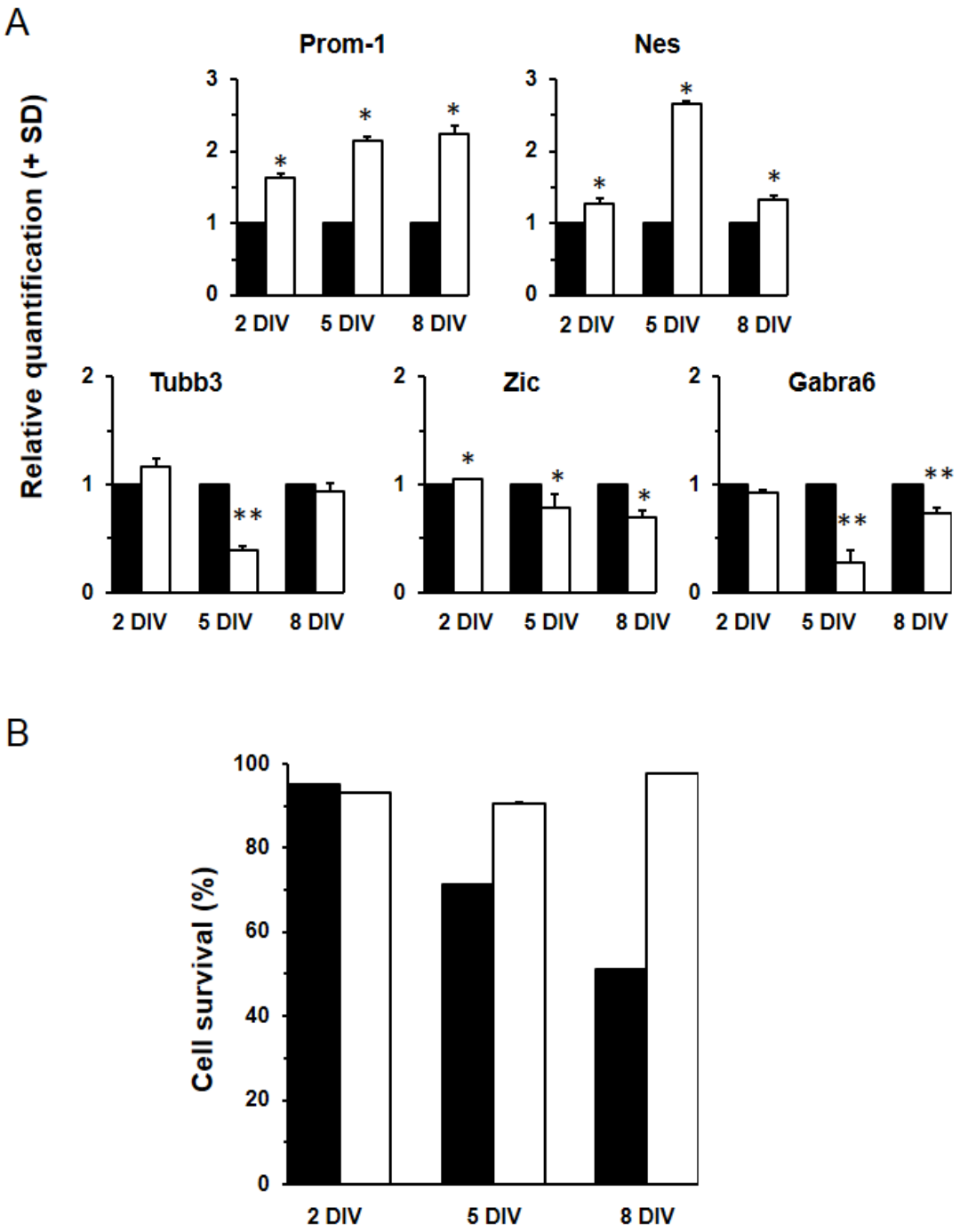

Figure 10. Lamin C knock down.
(**A**) Levels of the indicated mRNA in LMNA-KD GCs (white). The data are reported as the level of mRNA relative to the respective GCs-CTR (black) and are the mean+SD (n = 5). Statistical significance, *p≤0.05; **p≤0.01.
(**B**) Effect of silencing of LMNA gene on glutamate sensitivity. At 2, 5 and 8 DIV Mock (black) and LMNA-KD GCs (white) were treated with 10 mM glutamate in Locke solution for 30 min and then reincubated in their fresh medium serum free for 18 h. Data represent the means + standard deviation (s.d.; n = 5) of viable cells calculated as the ratio (%) between intact nuclei counted after the glutamate pulse and those counted in a sister control culture. Statistical significance: ***p< 0.001.

5 DISCUSSION

In this thesis work I demonstrate that the down regulation of Lamin A/C expression in the SH-SY5Y NB cells allows the development of a tumor-initiating cell (TIC) population with self-renewal features and the ability to initiate tumors *in vivo*.

TICs have been identified in many tumor types as a small tumorigenic population of cells that are responsible for sustaining tumor growth and metastatic spread, thus representing the cause of cancer recurrence (Dalerba et al., 2007; Ward et al., 2007; Frank et al., 2010). Their presence has been demonstrated in the bone marrow of patients with relapsed NB (Hansford et al., 2007), and they have many stem cell characteristics, such as sphere-forming ability and self-renewal. However, sphere-forming ability is not a general characteristic of NB tumor-derived cell lines, as reported by Mahller and colleagues, who studied the capacity to give rise to spheres in eight NB cell lines, including SH-SY5Y (Mahller et al., 2009). In accordance with these authors, we also found that NB SH-SY5Y cells were not able to form spheres. However, when we silenced the LMNA gene in these cells, they gave rise to spheres in serum-free culture conditions that were optimized for neural stem cell growth. The capacity to form spheres clearly demonstrates that this selected population possesses the self-renewal characteristics of a stem cell phenotype. Pluripotency is a unique state in which cells can self-renew indefinitely while maintaining the ability to differentiate. The mechanism that controls the transcription of core pluripotency factors has been extensively studied (Kashyap et al., 2009; Loh et al., 2006). In normal embryonic stem cells, the gene regulatory networks of the core transcription factors Oct4, Nanog and Sox2 are involved in pluripotency maintenance (Loh et al., 2006). Consistently, we found that the three main genes belonging to the stem cell regulatory network (POU5f, which encodes Oct4, NANOG and SOX2) were all significantly overexpressed in LMNA-KD-derived tumor spheres and even more so when the sphere cell population was cultured as adherent cells.

In addition, the fact that these spheres are highly positive for the CD133 marker further supports the stem-like phenotype of LMNA-KD cells.

We also found in LMNA-KD-derived tumor spheres a marked increase in the expression of the ABC membrane transporter gene ABCG2. Increased expression of this gene is considered a major characteristic of the cancer stem cell population that is associated with different tumor types (Ding et al., 2010). The increased expression of this drug resistance-related gene often correlates with the presence of a side population (Zeng et al., 2009). Indeed, we found the unambiguous presence of a

side population completely abolished by the exposure to verapamil, a known inhibitor of the membrane drug efflux-pump, in LMNA-KD cells.

To corroborate further that this cell population with self-renewal characteristics was a TIC population, we studied the capacity of these cells to give rise to tumors. The analysis of tumor growth *in vivo* clearly demonstrated that the putative TICs were more markedly aggressive, as evidenced by their higher growth rate at low cell concentrations than the LMNA-KD whole cell population and by the more malignant phenotype of the tumor tissues. The aggressiveness of the TIC population was also evidenced by increase of ENPP2 and decrease of EDN1 and CD44 gene expression. We can therefore conclude that the LMNA-KD sphere-derived cells represent a TIC population.

The inverse relationship between LMNA and MYCN found in the TICs indicate that these two genes can mutually regulate differentiation and stemness in NB. Indeed, TICs which express more MYCN than SH-SY5Y control cells and are silenced for LMNA gene, also show a significant increase of the NANOG, POU5f and SOX2 gene expression. This is supported by the data obtained from biopsies of human NB. Indeed, we found, for the first time in this paper, a defined inverse relationship between LMNA and MYCN gene expression in 23 human NB biopsies.

On the other hand, the miRNome analysis in two NB cellular model expressing LMNA or MYCN alternatively, evidenced changes of members of miRNA signatures which control cell proliferation and differentiation. In fact, in the SH-SY5Y LMNA expressing cells DAVID pathway analysis revealed that the miRNA target genes identified by DIANA bioinformatic tool belonged mainly to pathways related to cell cycle regulation indicating that the expression of Lamin A/C is associated with a more mature phenotype. This confirm data of a previous paper from our laboratory where we demonstrated that LMNA knock-down inhibit differentiation processes. By the contrary, in the LAN-5 MYCN expressing cells the miRNA target genes identified belonged to pathways related to the inhibition of the developmental processes. In particular, some of these genes (SMAD2, SMAD3, FGF2) appear to be involved in stem cell differentiation processes (Eom et al., 2014). The very different number of miRNAs identified in each cluster comparing the two cell lines support our hypothesis. It is likely that miRNAs and their target genes in LAN-5 cells tend to display a low number of clusters as a consequence of reduced number of pathways to be regulated to maintain their stem-like phenotype. By contrast, SH-SY5Y cells need to control a higher number of pathways than LAN-5 cells, due to their more mature phenotype. On the other hand, it is important to highlight that the analysis has been performed considering uniquely validated target.

Indeed, by up-regulating MYCN, through miR-101 modulation, in SH-SY5Y control cells, they acquired a stem-like phenotype; while down-regulating MYCN in LMNA-KD cells, we were able to restore a more mature phenotype. On the other hand, overexpression of the MYCN gene correlates with increased stemness characteristics (Kelly et al., 2000; Knoepfler et al., 2008; Ramalho-Santos, 2002). In addition, the role of the MYCN gene in promoting tumor invasion, particularly in NB cells, is well known (Tanaka et al., 2008; Hasan et al., 2013; Megison et al., 2013)

Our data provide new mechanistic insight into the development of a stem-like NB TIC population. In a tumor-mass, TICs constitute a rare tumorigenic cell population responsible for sustaining tumor growth, metastases and relapse. Our data may provide opportunities to develop new personalized therapeutic strategies based on the molecular profile of the tumor.

These data are further supported by the results obtained in the granule normal cells. In fact, I demonstrate that Lamin A/C may have a role in GCs maturation processes. The maturation and differentiation of GCs is promoted by excitatory amino acids receptors activation, such as glutamate.

The primary cultures of GCs have a short life, in fact as their maturation progresses become gradually more and more vulnerable to the effect of glutamate, and after eight days of culture they reach their full maturity and die by necrosis (Ankarcrona et al., 1995). Lamin A/C knock down prevents glutamate-mediated neuronal death and, as consequence, the complete maturation of GCs.

The contribute of A-type lamins to the capacity for postsynaptic plasticity inherent to excitatory synapses is mediated by interaction with Nesprins. Nesprin-1 isoform (called also CPG2, syne-1, myne-1, and Enaptin) is a critical component of the postsynaptic endocytic pathway that mediates both constitutive and activity-regulated glutamate receptor internalization (Cottrell et al., 2004). LMNA knock down seems to disrupt the constitutive internalization of glutamate receptors.

We therefore assume that Lamin A/C is a key component of neuronal plasticity.

6 BIBLIOGRAFY

Adolph K. W., (1987) **ADPribosylation of nuclear proteins labeled with [3H]adenosine: changes during the HeLa cycle.** *Biochim Biophys Acta* 909(3): 222-230.

Aebi U., et al., (1986). **The nuclear lamina is a meshwork of intermediate-type filaments.** *Nature* 323: 560-564.

Agrelo R., et al., (2005) **Inactivation of the lamin A/C gene by CpG island promoter hypermethylation in hematologic malignancies, and its association with poor survival in nodal diffuse large B-cell lymphoma.** *Clin Oncol* 23(17): 3940-3947.

Al-Hajj M., et al., (2003) **Prospective identification of tumorigenic breast cancer cells.** *Proc Natl Acad Sci USA* 100(7): 3983-3988.

Alsheimer M. and Benavente R., (1996) **Change of Karyoskeleton during Mammalian Spermatogenesis: Expression Pattern of Nuclear Lamin C2 and its Regulation**. *Exp Cell Res* 228(2): 181-188.

Ambros V., et al., (2003) **A uniform system for microRNA annotation.** *RNA* 9(3): 277-279.

Ankarcrona M., et al., (1995) **Glutamate-induced neuronal death: a succession of necrosis or apoptosis depending on mitochondrial function.** *Neuron* 15(4): 961-973.

Arora P., et al., (2004) **Cell-type-specific interactions at regulatory motifs in the first intron of the lamin A gene.** *FEBS Lett* 568(1-3): 122-128.

Bao S., et al., (2006) **Glioma stem cells promote radioresistance by preferential activation of the DNA damage response.** *Nature* 444(7120): 756-760.

Bartel D. P., (2004) **MicroRNAs: genomics, biogenesis, mechanism, and function.** *Cell* 116(2): 281-297.

Bartel D. P., (2009) **MicroRNAs: target recognition and regulatory functions.** *Cell* 136(2): 215-233.

Bonnet D. and Dick J.E., (1997) **Human acute myeloid leukemia is organized as a hierarchy that originates from a primitive hematopoietic cell.** *Nat Med* 3(7): 730-737.

Bridger J. M., et al., (1993) **Internal Lamin Structures within G1 Nuclei of Human Dermal Fibroblasts**. *J Cell Sci* 104: 297-306.

Brodeur G. M., (2003) **Neuroblastoma: biological insights into a clinical enigma.** *Nat Rev Cancer* 3(3): 203-216.

Broers J. L., et al., (1993) **Nuclear A-type lamins are differentially expressed in human lung cancer subtypes.** *Am J Pathol* 143(1): 211-220.

Broers J. L., et al., (1999) **Dynamics of the Nuclear Lamina as Monitored by GFP-Tagged A-Type Lamins** *J Cell Sci* 112(20): 3463-3475.

Broers J. L., et al., (2006) **Nuclear lamins: laminopathies and their role in premature ageing.** *Physiol Rev* 86(3): 967-1008.

Bruce W. R, Van der Gaag H., (1963) **A quantitative assay for the number of murine lymphoma cells capable of proliferation in vivo.** *Nature* 199: 79-80.

Buechner J., et al., (2011) **Tumour-suppressor microRNAs let-7 and mir-101 target the proto-oncogene MYCN and inhibit cell proliferation in MYCN-amplified neuroblastoma.** *Br J Cancer* 105(2): 296-303.

Burke B. and Gerce L., (1986) **A Cell Free System to Study Reassembly of the Nuclear Envelope at the End of Mitosis**. *Cell* 44(4): 639-652.

Buzzeo M. P., et al., (2007) **The hunt for cancer-initiating cells: a history stemming from leukemia.** *Leukemia* 21(8): 1619-1627.

Calin G. A. and Croce. C. M., (2006) **MicroRNA signatures in human cancers.** *Nat Rev Cancer* 6(11): 857-866.

Capell B. C. and Collins F. S., (2006) **Human laminopathies: nuclei gone genetically awry.** *Nat Rev Genet* 7(12): 940-952.

Chen X., et al., (2008) **Characterization of microRNAs in serum: a novel class of biomarkers for diagnosis of cancer and other diseases.** *Cell Res* 18(10): 997-1006.

Chen Y. and Stallings R. L., (2007) **Differential patterns of microRNA expression in neuroblastoma are correlated with prognosis, differentiation, and apoptosis.** *Cancer Res* 67(3): 976-983.

Christoffersen N. R., et al., (2010) **p53-independent upregulation of miR-34a during oncogene-induced senescence represses MYC.** *Cell Death Differ* 17(2): 236-245.

Clarke M. F., et al., (2006) **Cancer stem cells-perspectives on current status and future directions: AACR Workshop on cancer stem cells.** *Cancer Res* 66(19): 9339-9344.

Cloonan N., et al., (2008) **The miR-17-5p microRNA is a key regulator of the G1/S phase cell cycle transition.** *Genome Biol* 9(8): R127.

Constantinescu D., et al., (2006) **Lamin A/C expression is a marker of mouse and human embryonic stem cell differentiation.** *Stem Cells* 24(1): 177-185.

Coradeghini R., et al., (2006) **Differential expression of nuclear lamins in normal and cancerous prostate tissues.** *Oncol Rep* 15(3): 609-613.

Cottrell J. R, et al., (2004) **CPG2: a brainand synapse-specific protein that regulates the endocytosis of glutamate receptors.** *Neuron* 44(4): 677-690.

Crisp M., et al., (2006) **Coupling of the nucleus and cytoplasm: role of the LINC complex.** *J Cell Biol* 172(1): 41-53.

Dalerba P., Cho R. W. and Clarke M. F., (2007) **Cancer stem cells: models and concepts.** *Annu Rev Med* 58: 267-284.

Dalerba P., et al., (2007) **Phenotypic characterization of human colorectal cancer stem cells.** *Proc Natl Acad Sci USA* 104(24): 10158-10163.

Davies B.S., et al., (2009) **The posttranslational processing of prelamin A and disease.** *Annu Rev Genomics Hum Genet* 10: 153-174.

Dechat T., et al., (2000) **Lamina-associated polypeptide 2alpha binds intranuclear A-type lamins.** *J Cell Sci* 113(19): 3473-3484.

Dechat T., et al., (2008) **Nuclear Lamins: Major Factors in the Structural Organisation and Function of the Nucleus and Chromatin.** *Genes Dev* 22(7): 832-853.

Dick J. E., (1991) **Immune-deficient mice as models for human hematopoietic disease.** *Cancer Cells* 3(2): 39-48.

Diehn M. and Clarke M. F., (2006) **Cancer stem cells and radiotherapy: new insights into tumor radioresistance.** *J Natl Cancer Inst* 98(24): 1755-1757.

Ding X. W., et al., (2010) **ABCG2: a potential marker of stem cells and novel target in stem cell and cancer therapy.** *Life Sci* 86(17-18): 631-637.

Dorner D., Gotzmann J. and Foisner R., (2007) **Nucleoplasmic Lamins and their Interaction Partners, LAP2alpha, Rb, and BAF, in Transcriptional Regulation.** *FEBS J* 274(6): 1362-1373.

Eiring A. M., et al., (2010) **miR-328 functions as an RNA decoy to modulate hnRNP E2 regulation of mRNA translation in leukemic blasts.** *Cell* 140(5): 652-665.

Eom Y. W., et al., (2014) **The role of growth factors in maintenance of stemness in bone marrow-derived mesenchymal stem cells.** *Biochem Biophys Res Commun* 445(1): 16-22.

Esiashvili N., et al., (2009) **Neuroblastoma.** *Curr Probl Cancer* 33(6): 333-360.

Esquela-Kerscher A., et al., (2008) **The let-7 microRNA reduces tumor growth in mouse models of lung cancer.** *Cell Cycle* 7(6): 759-764.

Etchevers H. C., Amiel J., Lyonnet S., (2006) **Molecular bases of human neurocrestopathies.** *Adv Exp Med Biol* 589: 213-234.

Fábián A., et al., (2009) **Die hard: are cancer stem cells the Bruce Willises of tumor biology?** *Cytometry A* 75(1): 67-74.

Favreau C., et al., (2004) **Expression of a mutant lamin A that causes Emery-Dreifuss muscular dystrophy inhibits in vitro differentiation of C2C12 myoblasts**. *Mol Cell Biol* 24(4): 1481-1492.

Ferraro A., et al., (1989) **Glycosylated forms of nuclear lamins.** *FEBS Lett* 257(2): 241-246.

Foisner R. and Gerace L., (1993) **Integral Membrane Proteins of the Nuclear Envelope Interact with Lamins and Chromosomes, and Binding is Modulated by Mitotic Phosphorylation.** *Cell* 73 (7): 1267-1279.

Foisner R., (2002) **Dynamic Connections of Nuclear Envelope Proteins to Chromatin and the Nuclear Matrix.** in Collas P. "Nuclear Envelope Dynamics in Embryos and Somatic Cells", chapter 4: 43-59.

Fontana L., et al., (2008) **Antagomir-17-5p abolishes the growth of therapy-resistant neuroblastoma through p21 and BIM.** *PLoS One* 3(5): e2236.

Foster H. A., and Bridger J. M., (2005) **The Genome and the Nucleus: A Marriage Made by Evolution. Genome Organisation and Nuclear Architecture.** *Chromosoma* 114(4): 212-229.

Foster HA et al., (2007) **Lamins A and C are Present in the Nuclei of Early Porcine Embryos, with Lamin A being Distributed in Large Intranuclear Foci.** *Chromosome Res* 15(2): 163-174.

Frangioni J. V., et al., (1993) **Use of a general purpose mammalian expression vector for studying intracellular protein targeting: identification of critical residues in the nuclear lamin A/C nuclear localization signal.** *J Cell Sci* 105: 481-488.

Frank N. Y., Schatton T. and Frank M. H., (2010) **The therapeutic promise of the cancer stem cell concept.** *J Clin Invest* 120: 41-50.

Friedman R. C., et al., (2009) **Most mammalian mRNAs are conserved targets of microRNAs.** *Genome Res* 19(1): 92-105.

Frock R. L., et al., (2006) **Lamin A/C and emerin are critical for skeletal muscle satellite cell differentiation.** *Genes Dev.* 20(4): 486-500.

Furukawa K. and Kondo T., (1998), **Identification of the Lamina-Associated-Polypeptide-2-Binding Domain of B-type Lamin**, *Eur J Biochem* 251(3): 729-733.

Gal H. G., et al., (2008) **MIR-451 and Imatinib mesylate inhibit tumor growth of Glioblastoma stem cells**. *Biochem Biophys Res Commun* 376(1): 86-90.

Garzia L., et al., (2009) **MicroRNA-199b-5p impairs cancer stem cells through negative regulation of HES1 in medulloblastoma.** *PLoS One* 4(3): e4998.

Gerace L. and Blobel G., **(**1980) **The nuclear envelope lamina is reversibly depolymerized during mitosis.** *Cell* 19(1): 277-287.

Gerace L. and Burke B., (1998) **Functional organization of the nuclear envelope.** *Annu Rev Cell Biol* 4: 335-374.

Gil J., et al., (2008) **Cancer stem cells: the theory and perspectives in cancer therapy.** *J Appl Genet* 49(2): 193-199.

Godlewski J., et al., (2008) **Targeting of the Bmi-1 oncogene/stem cell renewal factor by microRNA-128 inhibits glioma proliferation and self-renewal.** *Cancer Res* 68(22): 9125-9130.

Goldberg M. W., et al., (2008) **Filaments made from A and B-type lamins differ in structure and organization.** *J Cell Sci* 121(2): 215-225.

Goldberg M., et al., (1999) **The tail domain of lamin Dm0 binds histones H2A and H2B.** *Proc Natl Acad Sci USA* 96(6): 2852-2857.

Greene N. D. and Copp A. J., (2009) **Development of the vertebrate central nervous system: formation of the neural tube.** *Prenat Diagn* 29(4): 303-311.

Gregory P. A., et al., (2008) **The miR-200 family and miR-205 regulate epithelial to mesenchymal transition by targeting ZEB1 and SIP1.** *Nat Cell Biol* 10(5): 593-601.

Griffiths-Jones S., et al., (2006) **miRBase: microRNA sequences, targets and gene nomenclature.** *Nucleic Acids Res* 34: D140-D144.

Guarnieri D. J. and DiLeone R. J., (2008) **MicroRNAs: a new class of gene regulators.** *Ann Med* 40(3): 197-208.

Guglielmi L., et al., (2014) **MYCN gene expression is required for the onset of the differentiation programme in neuroblastoma cells.** *Cell Death Dis.* 5(2): e1081.

Hansford L.M., et al., (2007) **Neuroblastoma cells isolated from bone marrow metastases contain a naturally enriched tumor-initiating cell.** *Cancer Res* 67(23): 11234-11243.

Haque F., et al., (2006) **SUN1 interacts with nuclear lamin A and cytoplasmic nesprins to provide a physical connection between the nuclear lamina and the cytoskeleton.** *Mol Cell Biol* 26(10): 3738-3751.

Hasan M. K., et al., (2013) **ALK is a MYCN target gene and regulates cell migration and invasion in neuroblastoma.** *Sci Rep* 3: 3450.

He L., et al., (2005) **A microRNA polycistron as a potential human oncogene.** *Nature* 435: 828-833.

Hermann P. C., et al., (2007) **Distinct populations of cancer stem cells determine tumor growth and metastatic activity in human pancreatic cancer.** *Cell Stem Cell* 1(3): 313-323.

Hoehner J. C., et al., (1998) **Developmental gene expression of sympathetic nervous system tumors reflects their histogenesis.** *Lab Invest* 78(1): 29-45.

Höger T. H., Krohne G. and Kleinschmidt J. A., (1991), **Interaction of Xenopus Lamins A and LII with chromatin in vitro Mediated by a Sequence Element in the Carboxyterminal Domain**, *Exp Cell Res* 197(2): 280-289.

Hong L., et al., (2010) **The miR-17-92 cluster of microRNAs confers tumorigenicity by inhibiting oncogene-induced senescence.** *Cancer Res* 70(21): 8547-8557.

Huang Y., et al., (2011) **Biological functions of microRNAs: a review.** *J Physiol Biochem* 67(1): 129-139.

Hubner S., et al., (2006) **Laminopathy-inducing lamin A mutants can induce redistribution of lamin binding proteins into nuclear aggregates.** *Exp Cell Res* 312(2): 171-183.

Hutchison C. J., (2002) **Lamins: Building Blocks or Regulators of Gene Expression?** *Nat Rev Mol Cell Biol* 3(11): 848-858.

Janaki Ramaiah M. and Parnaik V. K., (2006) **An essential GT motif in the lamin A promoter mediates activation by CREB-binding protein.** *Biochem Biophys Res Commun* 348(3): 1132-1137.

Ji J., et al., (2009) **Identification of microRNA-181 by genome-wide screening as a critical player in EpCAM-positive hepatic cancer stem cells.** *Hepatology* 50: 472-480.

Ji Q., et al., (2008) **Restoration of tumor suppressor miR-34 inhibits human p53-mutant gastric cancer tumorspheres.** *BMC Cancer* 8: 266.

Ji Q., et al., (2009) **MicroRNA miR-34 inhibits human pancreatic cancer tumor-initiating cells.** *PLoS One* 4(8): e6816.

Jones R. J., Matsui W. H. and Smith B. D., (2004) **Cancer stem cells: are we missing the target?** *J Natl Cancer Inst* 96(8): 583-585.

Kashyap V., et al., (2009) **Regulation of stem cell pluripotency and differentiation involves a mutual regulatory circuit of the NANOG, OCT4, and SOX2 pluripotency transcription factors with polycomb repressive complexes and stem cell microRNAs.** *Stem Cells Dev* 18(7): 1093-1108.

Kasinski A. L. and Slack. F. J., (2011) **Epigenetics and genetics. MicroRNAs en route to the clinic: progress in validating and targeting microRNAs for cancer therapy.** *Nat Rev Cancer* 11(12): 849-864.

Kelly D. L. and Rizzino A., (2000) **DNA microarray analyses of genes regulated during the differentiation of embryonic stem cells.** *Mol Reprod Dev* 56(2): 113-123.

Ketema M., et al., (2007) **Requirements for the localization of nesprin-3 at the nuclear envelope and its interaction with plectin.** *J Cell Sci* 120(19): 3384-3394.

Kim V. N., Han J. and Siomi M. C., (2009) **Biogenesis of small RNAs in animals.** *Nat Rev Mol Cell Biol* 10(2): 126-139.

Knoepfler P. S., (2008) **Why myc? An unexpected ingredient in the stem cell cocktail.** *Cell Stem Cell* 2(1): 18-21.

Kong W., et al., (2008) **MicroRNA-155 is regulated by the transforming growth factor beta/Smad pathway and contributes to epithelial cell plasticity by targeting RhoA**. *Mol Cell Biol* 28(22): 6773-6784.

Kozomara A. and Griffiths-Jones S., (2011) **miRBase: integrating microRNA annotation and deepsequencing data.** *Nucleic Acids Res* 39: D152-D157.

LaBonne C. and Bronner-Fraser M., (1999) **Molecular mechanisms of neural crest formation.** *Annu Rev Cell Dev Biol* 15: 81-112.

Laszlo J., (1965) **Cancer chemotherapy for practicing physicians.** *J Chronic Diseases* 18(7): 681-687.

Lewis B. P., Burge C. B. and Bartel D. P., (2005) **Conserved seed pairing, often flanked by adenosines, indicates that thousands of human genes are microRNA targets.** *Cell* 120(1): 15-20.

Li C., et al., (2007) **Identification of pancreatic cancer stem cells.** *Cancer Res* 67(3): 1030-1037.

Li J., et al., (2015) **The role of miR-205 in the VEGF-mediated promotion of human ovarian cancer cell invasion.** *Gynecol Oncol* 137(1): 125-133.

Lin F. and Worman H. J., (1993) **Structural Organization of the Human Gene Encoding Nuclear Lamin A and Nuclear Lamin C**. *J Biol Chem* 268(22): 16321-16326.

Lin F. and Worman H. J., (1995) **Structural Organization of the Human Gene (LMNB1) Encoding Nuclear Lamin B1**. *Genomics* 27(2): 230-236.

Lin F. and Worman H. J., (1997) **Expression of Nuclear Lamins in Human Tissues and Cancer Cell Lines and Transcription from the Promoters of The Lamin A/C and B1 Genes.** *Exp Cell Res* 236(2): 378-384.

Lloyd D. J., Trembath R. C. and Shackleton S., (2002) **A novel interaction between lamin A and SREBP1: implications for partial lipodystrophy and other laminopathies.** *Hum Mol Genet* 11(7): 769-777.

Loh Y. H., et al., (2006) **The Oct4 and Nanog transcription network regulates pluripotency in mouse embryonic stem cells.** *Nat Genet* 38(4): 431-440.

Lu J., et al., (2005) **MicroRNA expression profiles classify human cancers.** *Nature* 435(7043): 834-838.

Ma L., et al., (2010) **Therapeutic silencing of miR-10b inhibits metastasis in a mouse mammary tumor model.** *Nat Biotechnol* 28(4): 341-347

Machiels B. M., et al., (1997) **Nuclear lamin expression in normal testis and testicular germ cell tumours of adolescents and adults.** *J Pathol* 182(2): 197-204.

Macingová Z. and Filip S., (2008) **Cancer stem cells--new approach to cancerogenensis and treatment.** *Acta Medica (Hradec Kralove)* 51(3): 139-144.

Mahller Y. Y., et al., (2009) **Neuroblastoma cell lines contain pluripotent tumor initiating cells that are susceptible to a targeted oncolytic virus.** *PLoS One* 4(1): e4235.

Margalit A., et al., (2007) **Barrier to autointegration factor blocks premature cell fusion and maintains adult muscle integrity in C. elegans.** *J.Cell Biol* 178(4): 661-673.

Maris J. M., (2010) **Recent advances in neuroblastoma.** *N Engl J Med* 362(23): 2202-2211.

Martin C., et al., (2009) **Lamin B1 Maintains the Functional Plasticity of Nucleoli.** *J Cell Sci* 122(10): 1551-1562.

Mattout, A., et al., (2007) **Specific and conserved sequences in D. melanogaster and C. elegans lamins and histone H2A mediate the attachment of lamins to chromosomes.** *J Cell Sci* 120(1): 77-85.

Mattout-Drubezki A. and Gruenbaum Y., (2003) **Dynamic Interactions of Nuclear Lamina Proteins with Chromatin and Transcriptional Machinery.** *Cell Mol Life Sci* 60(10): 2053-2063.

Megison M. L., et al., (2013) **FAK inhibition decreases cell invasion, migration and metastasis in MYCN amplified neuroblastoma.** *Clin Exp Metastasis* 30(5): 555-568.

Mendell J. T., (2008) **miRiad roles for the miR-17-92 cluster in development and disease.** *Cell* 133(2): 217-222.

Mitchell P. S., et al., (2008) **Circulating microRNAs as stable bloodbased markers for cancer detection.** *Proc Natl Acad Sci USA* 105: 10513-10518.

Modak S., Cheung N. V., (2010) **Neuroblastoma: Therapeutic strategies for a clinical enigma.** *Cancer Treat Rev* 36(4): 307-317.

Moss S. F., et al., (1999) **Decreased and aberrant nuclear lamin expression in gastrointestinal tract neoplasms.** *Gut* 45(5): 723-729.

Mueller S. and Matthay K. K., (2009) **Neuroblastoma: biology and staging.** *Curr Oncol Rep* 11(6): 431-438.

O'Brien C. A., et al., (2007) **A human colon cancer cell capable of initiating tumour growth in immunodeficient mice.** *Nature* 445(7123): 106-110.

Oguchi M., et al., (2002) **Expression of lamins depends on epidermal differentiation and transformation.** *Br J Dermato* 147(5): 853-858.

Okumura K., et al., (2000) **Identification of a novel retinoic acid-responsive element within the lamin A/C promoter.** *Biochem Biophys Res Commun* 269(1): 197-202.

Okumura K., Hosoe Y. and Nakajima N., (2004) **c-Jun and Sp1 family are critical for retinoic acid induction of the lamin A/C retinoic acid-responsive element.** *Biochem Biophys Res Commun* 320(2): 487-492.

Ottaviano Y. and Gerace L., (1985) **Phosphorylation of the nuclear lamins during interphase and mitosis.** *J Biol Chem* 260(1): 624-632.

Padmakumar V. C., et al., (2005) **The inner nuclear membrane protein Sun1 mediates the anchorage of Nesprin-2 to the nuclear envelope.** *J Cell Sci* 118(15): 3419-3430.

Pallini R., et al., (2008) **Cancer stem cell analysis and clinical outcome in patients with glioblastoma multiforme.** *Clin Cancer Res* 14(24): 8205-8212.

Park N. J., et al., (2009) **microRNA: discovery, characterization, and clinical utility for oral cancer detection.** *Clin Cancer Res* 15(17): 5473-5477.

Park S. M., et al., (2008) **The miR-200 family determines the epithelial phenotype of cancer cells by targeting the E-cadherin repressors ZEB1 and ZEB2.** *Genes Dev* 22(7): 894-907.

Patrawala L., et al., (2005) **Side population is enriched in tumorigenic, stem-like cancer cells, whereas ABCG2+ and ABCG2- cancer cells are similarly tumorigenic.** *Cancer Res* 65(14): 6207-6219.

Piccirillo S. G., et al., (2006) **Bone morphogenetic proteins inhibit the tumorigenic potential of human brain tumour-initiating cells.** *Nature* 444(7120): 761-765.

Poliseno L., et al., (2010) **A coding-independent function of gene and pseudogene mRNAs regulates tumour biology.** *Nature* 465(7301): 1033-1038.

Prather R. S., et al., (1989) **Nuclear Lamin Antigens are Developmentally Regulated during Porcine and Bovine Embryogenesis.** *Biol Reprod* 41(1): 123-132.

Quintana E., et al., (2008) **Efficient tumour formation by single human melanoma cells.** *Nature* 456(7222): 593-598.

Ramalho-Santos M., et al., (2002) **"Stemness": transcriptional profiling of embryonic and adult stem cells.** *Science* 298(5593): 597-600.

Razafsky D., et al., (2014) **Nuclear envelope in nuclear positioning and cell migration.** *Adv Exp Med Biol* 773: 471-490.

Rettig W. J., et al., (1987) **Coordinate changes in neuronal phenotype and surface antigen expression in human neuroblastoma cell variants.** *Cancer Res* 47(5): 1383-1389.

Rhodes G., et al., (2010) **Lamin B Receptor: Multi-Tasking at the Nuclear Envelope**, *Nucleus* 1(1): 53-70.

Rosen J. M. and Jordan C. T., (2009) **The increasing complexity of the cancer stem cell paradigm.** *Science* 324(5935): 1670-1673.

Ross R. A. and Spengler B. A., (2007) **Human neuroblastoma stem cells.** *Semin Cancer Biol* 17(3): 241-247.

Ross R. A., Biedler J. L. and Spengler B. A., (2003) **A role for distinct cell types in determining malignancy in human neuroblastoma cell lines and tumors.** *Cancer Lett* 197(1-2): 35-39.

Ross R. A., et al., (1995) **Human neuroblastoma I-type cells are malignant neural crest stem cells.** *Cell Growth Differ* 6(4): 449-456.

Salmena L., et al., (2011) **A ceRNA hypothesis: the Rosetta Stone of a hidden RNA language?** *Cell* 146(3): 353-358.

Sasse B., Aebi U. and Stuurman N., (1998) **A tailless Drosophila lamin Dm0 fragment reveals lateral associations of dimers.** *J Struct Biol* 123(1): 56-66.

Schatton T., et al., (2008) **Identification of cells initiating human melanomas.** *Nature* 451(7176): 345-349.

Schirmer E. C. and Foisner R., (2007) **Proteins that associate with lamins: many faces, many functions.** *Exp Cell Res* 313(10): 2167-2179.

Seeger R. C., et al., (1985) **Association of multiple copies of the N-myc oncogene with rapid progression of neuroblastomas.** *N Engl J Med* 313(18): 1111-1116.

Shackleton M., et al., (2009) **Heterogeneity in cancer: cancer stem cells versus clonal evolution.** *Cell* 138(5): 822-829.

Shimono Y., et al., (2009) **Downregulation of miRNA-200c links breast cancer stem cells with normal stem cells.** *Cell* 138(3): 592-603.

Singh S. K., et al., (2004) **Identification of human brain tumour initiating cells.** *Nature* 432(7015): 396-401.

Siomi H. and Siomi M. C., (2009) **On the road to reading the RNA-interference code.** *Nature* 457(7228): 396-404.

Stadelmann B., et al., (1990) **Repression of nuclear lamin A and C gene expression in human acute lymphoblastic leukemia and non-Hodgkin's lymphoma cells.** *Leuk Res* 14(9): 815-821.

Takahashi Y., et al., (2013) **Orexin neurons are indispensable for prostaglandin E2-induced fever and defence against environmental cooling in mice.** *J Physiol* 591(22): 5623-5643.

Takamori Y., et al., (2007) **Differential expression of nuclear lamin, the major component of nuclear lamina, during neurogenesis in two germinal regions of adult rat brain.** *Eur J Neurosci* 25(6): 1653-1662.

Tanaka N. and Fukuzawa M., (2008) **MYCN downregulates integrin alpha1 to promote invasion of human neuroblastoma cells.** *Int J Oncol* 33(4): 815-821.

Tang D. G., et al., (2007) **Prostate cancer stem/progenitor cells: identification, characterization, and implications.** *Mol Carcinog* 46(1): 1-14.

Tay Y., et al., (2008) **MicroRNAs to Nanog, Oct4 and Sox2 coding regions modulate embryonic stem cell differentiation.** *Nature* 455(7216): 1124-1128.

Tilli C. M., et al., (2003) **Lamin expression in normal human skin, actinic keratosis, squamous cell carcinoma and basal cell arcinoma.** *Br J Dermatol* 148(1): 102-109.

Vasudevan S., Tong Y. and Steitz J. A., (2007) **Switching from repression to activation: microRNAs can up-regulate translation.** *Science* 318(5858): 1931-1934.

Venables R. S., et al., (2001) **Expression of individual lamins in basal cell carcinomas of the skin.** *Br J Cancer* 84(4): 512-519.

Verstraeten V. L., et al., (2007) **The nuclear envelope, a key structure in cellular integrity and gene expression.** *Curr Med Chem* 14(11): 1231-1248.

Vescovi A. L., (2006) **Brain tumour stem cells.** *Nat Rev Cancer* 6(6): 425-436.

Visvader, J. E. and Lindeman G. J., (2008) **Cancer stem cells in solid tumours: accumulating evidence and unresolved questions.** *Nat Rev Cancer* 8(10): 755-768.

Vlachos S., et al., (2014) **DIANA-TarBase v7.0: indexing more than half a million experimentally supported miRNA:mRNA interactions.** *Nucleic Acids Res* 43: D153-D159.

Vlcek S., Dechat T. and Foisner R., (2001) **Nuclear Envelope and Nuclear Matrix: Interactions and Dynamics**. *Cell Mol Life Sci* 58(12-13): 1758-1765.

Walton J. D., Kattan R. D. and Ross R. A., (2004) **Characteristics of Stem Cells from human neuroblastoma cell lines and in tumors.** *Neoplasia* 6(6): 838-845.

Wang H. R., et al., (2003) **Regulation of cell polarity and protrusion formation by targeting RhoA for degradation.** *Science* 302(5651): 1775-1779.

Ward R. J. and Dirks P. B., (2007) **Cancer stem cells: at the headwaters of tumor development.** *Annu Rev Pathol* 2: 175-189.

Warren D. T., et al., (2005) **Nesprins: intracellular scaffolds that maintain cell architecture and coordinate cell function?** *Expert Rev Mol Med* 7(11): 1-15.

Weber J. A., et al., (2010) **The microRNA spectrum in 12 body fluids.** *Clin Chem* 56(11): 1733-1741.

Wiche G., (1998) **Role of plectin in cytoskeleton organization and dynamics.** *J Cell Sci* 111(17): 2477-2486.

Wilson K. L. and Foisner R., (2010), **Lamin-binding Proteins**, *Cold Spring Harb Perspect Biol* 2(4): a000554.

Wydner K. L., et al., (1996) **Chromosomal assignment of human nuclear envelope protein genes LMNA, LMNB1, and LBR by fluorescence in situ hybridization.** *Genomics* 32(3): 474-478.

Ye Q. and Worman H. J., (1994) **Primary structure analysis and lamin B and DNA binding of human LBR, an integral protein of the nuclear envelope inner membrane**. *J Biol Chem* 269(15): 11306-11311.

Young S. G., et al., (2014) **Nuclear lamins and neurobiology.** *Mol Cell Biol* 34(15): 2776-2785.

Yu F., et al., (2007) **let-7 regulates self renewal and tumorigenicity of breast cancer cells.** *Cell* 131(6): 1109-1123.

Yu F., et al., (2010) **Mir-30 reduction maintains self-renewal and inhibits apoptosis in breast tumor-initiating cells.** *Oncogene* 29(29): 4194-4204.

Zavadil J., et al., (2007) **Transforming growth factor-β and microRNA:mRNA regulatory networks in epithelial plasticity.** *Cells Tissues Organs* 185(1-3): 157-161.

Zeng H., et al., (2009) **Lack of ABCG2 expression and side population properties in human pluripotent stem cells.** *Stem Cells* 27(10): 2435-2445.

Zhang Y. Q. and Sarge K. D., (2008) **Sumoylation regulates lamin A function and is lost in lamin A mutants associated with familial cardiomyopathies.** *J Cell Biol* 182(1): 35-39.

APPENDIX

Functional analysis of differentially and specifically expressed miRNAs performed by DIANA tool showing statistically over-represented groups in and LAN-5 (red) SH-SY5Y(green) cells.

Increased in LAN-5*

Term (KEGG_Pathway)	Count	miRNA|TarBase				Count	PValue	Target Genes							
hsa04110:Cell cycle	7	miR-376a-3p	miR-372	miR-193b-3p	miR-572	29	4.05E-32	ESPL1	CDC6	PCNA	E2F1	CCNB1	E2F2	CCNA2	MCM6
		miR-302d-3p	miR-942	miR-19a-3p				CDK1	CDK6	MCM7	CHEK1	CCND1	SMAD4	CCNE2	PKMYT1
								CDK2	CCND2	MCM4	MCM5	WEE1	ORC6	MCM3	CDC25A
								TTK	YWHAZ	CDC20	BUB1B	CDKN1A			
hsa05200:Pathways in cancer	11	miR-182-5p	miR-378a-5p	miR-383	miR-942	31	1.12E-08	E2F1	RAC2	E2F2	RAD51	TCF7L1	ETS1	BCL2	KRAS
		miR-193b-3p	miR-572	miR-19a-3p	miR-491-5p			MSH6	CCNE2	MAPK8	NFKB2	HSP90AB1	CASP9	MAX	EP300
		miR-372	miR-200c-3p	miR-302d-3p				CDK6	MITF	CDH1	CCND1	SMAD4	BCL2L1	LEF1	FN1
								VEGFA	PTEN	FOXO1	TGFBR2	CDKN1A	SUFU		
hsa04115:p53 signaling pathway	8	miR-494	miR-130b-5p	miR-372	miR-19a-3p	15	1.35E-05	CCNB1	CDK2	CCND2	CDK1	CDK6	CHEK1	CCND1	CCNE2
		miR-193b-3p	miR-572	miR-942	miR-302d-3p			RCHY1	CASP9	SESN2	CDKN1A	RRM2	PTEN	PPM1D	
hsa04110:PI3K-Akt signaling pathway	7	miR-494	miR-182-5p	miR-383		13	8.07E-03	CDK2	CCND2	BCL2	CCND1	CCNE2	BCL2L1	FOXO3	CDKN1A
		miR-372	miR-19a-3p	miR-302d-3p				VEGFA	PTEN	SGK3	PRKCZ	BCL2L11			
		miR-491-5p													
hsa05202:Transcriptional misregulation in cancer	6	miR-370	miR-372	miR-572	miR-486-5p	4	4.32E-02	HMGA2	CD40	BCL2L1	CDKN1A				
		miR-491-5p	miR-942												

Increased in SH-SY5Y*

Term (KEGG_Pathway)	Count	miRNA|TarBase				Count	PValue	Target Genes							
hsa04115:p53 signaling pathway	19	miR-214-3p	miR-449a	miR-24-3p	miR-34a-5p	44	1.08E-29	CCNG1	ZMAT3	CCNB1	SFN	CDK4	BID	MDM2	RFWD2
		miR-222-3p	miR-21-5p	miR-374a-5p	miR-503			THBS1	CDK2	CCND2	DDB2	CDK1	GADD45A	CCND3	CDKN2A
		miR-424-15p	miR-193a-5p	miR-30d-5p	miR-101-3p			CDK6	CHEK1	TP53	APAF1	ATM	PMAIP1	PIDD1	CASP3
		miR-26b-5p	miR-26a-5p	miR-93-5p	miR-363-3p			CCND1	CCNE2	TP73	EI24	SESN1	CASP9	PPM1D	SESN2
		miR-28-5p	miR-28-5p	miR-10a-5p				MDM4	FAS	BBC3	CASP8	SERPINB5	TP53I3	CCNG2	CCNE1
								CDKN1A	RRM2	SESN3	PTEN				
hsa05200:Pathways in cancer	25	miR-214-3p	let-7c	miR-21-5p	miR-449°	86	5.47E-24	FOS	GSK3B	STAT3	E2F1	TGFBR1	ERBB2	COL4A1	CDK4
		miR-34a-5p	miR-222-3p	let-7f-5p	let-7d-5p			STAT5A	E2F2	NRAS	CRKL	BID	TCF4	PDGFA	APC
		miR-503	miR-424-5p	miR-223-3p	miR-27a-3p			RUNX1	WNT1	HDAC1	WNT5A	HSP90AA1	RALA	MDM2	CHUK
		miR-29b-3p	miR-363-3p	miR-146b-3p	miR-93-5p			BCL2	CDKN1B	BIRC5	PLD1	IGF1R	EGFR	TFG	CDKN2A
		miR-26a-5p	miR-361-5p	miR-25-3p	miR-361-5p			APPL1	KRAS	CDK6	VHL	TP53	IKBKB	TGFBR2	PTK2
		miR-28-5p	miR-28-5p	miR-24-3p	miR-769-5p			FZD4	MMP2	MAPK9	AR	JUN	CCND1	FGF1	SMAD4
		miR-374a-5p						CTNNB1	MSH6	CCNE2	AXIN2	MMP1	SKP2	MAPK1	COL4A2
								E2F3	MAPK8	MYC	MMP9	MSH2	DAPK1	FOXO1	PDGFB
								NFKBIA	KIT	PIK3R1	RB1	RAC1	BMP2	FGFR1	FAS
								TGFB2	EP300	BCL2L1	CCNE1	LEF1	CDKN1A	PTEN	MAP2K1
								Il6	BIRC3	RALB	STAT1	ITGA6	VEGFA		
hsa04110:Cell cycle	19	let-7c	miR-449°	miR-24-3p	miR-100-5p	51	6.56E-21	ESPL1	CDC6	GSK3B	CDKN2C	PCNA	E2F1	CCND3	CCNB1
		miR-34a-5p	miR-222-3p	miR-28-5p	let-7d-5p			SFN	CDK4	E2F2	CDC14A	CCNA2	CDC25C	CDC25A	HDAC1
		let-7f-5p	miR-503	miR-28-5p	miR-424-5p			MCM6	CCND2	MCM4	ORC4	CDKN1B	MCM5	MDM2	STAG2
		miR-363-3p	miR-27a-3p	miR-374a-5p	miR-26a-5p			WEE1	CDK1	GADD45A	CDKN2A	CDK6	MCM7	MCM3	CHEK1
		miR-93-5p	miR-25-3p	miR-769-5p				TP53	ATM	CDKN1C	CCND1	SMAD4	CCNE2	ANAPC13	E2F5
								SKP2	E2F3	MYC	RB1	CDC20	CDC23	PLK1	EP300
								CCNE1	CDC27	CDKN1A					

hsa04110:PI3K-Akt signaling pathway	19	let-7c	miR-449a	miR-181c-5p	miR-100-5p	60	1.02E-07	GSK3B	CDK4	NRAS	FGFR3	MAP2K2	PIK3CB	BCL2L11	PPP2CA
		miR-222-3p	let-7d-5p	let-7f-5p	miR-503			CDC37	MCL1	CCND2	HSP90AA1	IFNB1	RAF1	CCND3	CHUK
		miR-424-5p	miR-29b-3p	miR-26a-5p	miR-7-5p			BCL2	CDKN1B	IGF1R	EGFR	GNB1	PPP2R5C	COL4A1	KRAS
		miR-146b-3p						CDK6	COL3A1	PAK1	IKBKB	DDIT4	CCND1	PDGFA	EIF4E
								CCNE2	COL4A2	PPP2R2A	MYC	PDGFB	COL1A1	MDM2	KIT
								HSP90B1	IRS1	RAC1	INSR	PRKAA1	CASP9	GNG5	BCL2L1
								PDGFC	CCNE1	FOXO3	CDKN1A	MAP2K1	LAMC2	PPP2R1B	COL5A3
								VEGFA	PTEN	FGFR1	FGF1				
hsa05202:Transcriptional misregulation in cancer	11	miR-34a-5p	miR-223-3p	miR-28-5p	miR-363-3p	41	3.14E-03	HIST1H3B	CDKN2C	HIST1H3A	BAIAP3	LMO2	HIST3H3	PAX3	RUNX1
		miR-27a-3p	miR-26a-5p	miR-101-3p	miR-146b-3p			HMGA2	HDAC1	CCND2	HOXA9	CDKN1B	HIST2H3C	MEIS1	IGF1R
		miR-93-5p	miR-25-3p					HIST1H3E	ZEB1	TP53	ATM	CEBPB	HIST1H3I	TGFBR2	MYC
								KLF3	HIST1H3C	PDGFB	H3F3A	HIST1H3H	SP1	GOLPH3	H3F3B
								MYCN	CDKN1A	Il6	BIRC3	MEF2C	FOXO1	HIST2H3A	SMAD1
								HIST1H3J							

(Increased in SH-SY5Y*)

differentially expressed at least 2-fold comparing the two cell lines.

Specific in LAN-5

Term (KEGG_Pathway)	Count	miRNA|TarBase				Count	PValue	Target Genes							
hsa05200:Pathways in cancer	6	miR-96-5p	miR-155-5p	miR-504	miR-654-3p	40	2,58E-07	GSK3B	STAT3	NFKB1	SPI1	CDK4	SMAD2	E2F2	Spi1
		miR-630	miR-639					APC	WNT5A	CDK2	BAX	Csf1r	ETS1	SMAD3	BCL2
								EGFR	RHOA	CDKN2A	KRAS	Hif1a	MLH1	MITF	SMAD4
								CTNNB1	MSH6	CTNNA1	COL4A2	MSH2	RAC1	FGF2	FAS
								NKX3-1	CDKN1A	VEGFA	FOXO1	CSF1R	FGF7	JUP	MDM2
hsa04115:p53 signaling pathway	4	miR-96-5p	miR-504	miR-654-3p	miR-639	4	7,77E-04	CCNB1	BAX	FAS	CDKN1A	MDM2			
hsa04110:PI3K-Akt signaling pathway	3	miR-221-3p	miR-302b-3p	miR-449b-5p	miR-34b-5p	30	7,38E-03	GSK3B	NFKB1	CDK4	THBS1	PPP2CA	CDK2	PCK2	Csf1r
		miR-126-5p	miR-34b-3p	miR-483-3p	miR-1285-3p			ITGB4	BCL2	EGFR	KRAS	RHEB	ITGB5	COL4A2	PPP2R2A
								FLT1	PDK1	YWHAZ	RAC1	FGF2	EIF4E2	FOXO3	PKN2
								CDKN1A	SGK3	CSF1R	FGF7	GNB4	BCL2L11		
hsa04110:Cell cycle	4	miR-155-5p	miR-654-3p	miR-639	miR-376a-5p	15	2,16E-02	GSK3B	CDK4	SMAD2	E2F2	CDK2	SMAD3	STAG2	WEE1
								CDKN2A	SMAD4	TTK	YWHAZ	CDKN1A	PRKDC	PLK1	

Specific in SH-SY5Y

Term (KEGG_Pathway)	Count	miRNA|TarBase	Count	PValue	Target Genes
hsa04110:Cell cycle	7	miR-221-3p miR-302b-3p miR-449b-5p miR-34b-5p miR-675-5p miR-34b-3p miR-483-3p	11	9,08E-10	CDK4 CCND2 CDKN1B CDK6 CDKN1C SMAD4 CCNE2 MYC RB1 CDC27 CDC25A
hsa05200:Pathways in cancer	5	miR-199b-5p miR-221-3p miR-449b-5p miR-34b-5p miR-34b-3p	12	5,24E-12	FOS CDK4 BCL2 CDKN1B CDK6 CCNE2 MYC KIT LAMC2 VEGFA PTEN DVL2
hsa04115:p53 signaling pathway	8	miR-221-3p miR-302b-3p miR-449b-5p miR-34b-5p miR-126-5p miR-34b-3p miR-483-3p miR-1285-3p	11	3,54E-11	CCNG1 CDK4 CCND2 CDK6 TP53 PMAIP1 CCNE2 SESN2 BBC3 SESN3 PTEN
hsa04110:PI3K-Akt signaling pathway	8	miR-181c-5p miR-199b-5p miR-221-3p miR-302b-3p miR-449b-5p miR-582-5p miR-34b-5p miR-34b-3p	20	1,52E-10	MYB CDK4 PPP2CA MCL1 CCND2 BCL2 CDKN1B GNB1 PPP2R5C KRAS CDK6 DDIT4 CCNE2 MYC KIT HSP90B1 FOXO3 LAMC2 VEGFA PTEN